# The search for new treatment strategies for malignant pleural mesothelioma

Schunselaar, L.M.

# Chapter 3

## Comprehensive Pharmacogenomic Profiling of Malignant Pleural Mesothelioma Identifies a Subgroup Sensitive to FGFR Inhibition.

Josine M.M.F. Quispel-Janssen*, Jitendra Badhai*, Laurel M. Schunselaar*, Stacey Price, Jonathan Brammeld, Francesco Iorio, Krishna Kolluri, Mathew Garnett, Anton Berns, Paul Baas, Ultan McDermott, Jacques Neefjes and Constantine Alifrangis
*equal contribution
Clin Cancer Res. 2018 Jan; 24(1):84-94

## Abstract

**Purpose**: Despite intense research, treatment options for patients with mesothelioma are limited and offer only modest survival advantage. We screened a large panel of compounds in multiple mesothelioma models and correlated sensitivity with a range of molecular features to detect biomarkers of drug response.

**Experimental design:** We utilized a high-throughput chemical inhibitor screen in a panel of 889 cancer cell lines, including both immortalized and primary early-passage mesothelioma lines, alongside comprehensive molecular characterization using Illumina whole-exome sequencing, copy-number analysis and Affymetrix array whole transcriptome profiling. Subsequent validation was done using functional assays such as siRNA silencing and mesothelioma mouse xenograft models.

**Results:** A subgroup of immortalized and primary MPM lines appeared highly sensitive to FGFR inhibition. None of these lines harbored genomic alterations of FGFR family members, but rather BAP1 protein loss was associated with enhanced sensitivity to FGFR inhibition. This was confirmed in a MPM mouse xenograft model and by BAP1 knockdown and overexpression in cell line models. Gene expression analyses revealed an association between BAP1 loss and increased expression of the receptors FGFR1/3 and ligands FGF9/18. BAP1 loss was associated with activation of MAPK signaling. These associations were confirmed in a cohort of MPM patient samples.

**Conclusion:** A subgroup of mesotheliomas cell lines harbor sensitivity to FGFR inhibition. BAP1 protein loss enriches for this subgroup and could serve as a potential biomarker to select patients for FGFR inhibitor treatment. These data identify a clinically relevant MPM subgroup for consideration of FGFR therapeutics in future clinical studies.

## Keywords

mesothelioma, FGFR, BAP1, biomarker

## Translational relevance

Malignant pleural mesothelioma (MPM) has limited treatment options and a dismal prognosis. To date, targeted therapies have proved ineffective, and no druggable genetic alterations have been identified. Selecting compounds for further clinical evaluation in this small and heterogeneous patient group is challenging. By combining high-throughput drug screens, comprehensive molecular characterization and functional assays in multiple mesothelioma models, we were able to identify an FGFR inhibitor-sensitive subgroup with BAP1 loss as a potential predictive biomarker. Loss of BAP1 is found in up to 64% of MPM tumors. These data suggest that a significant group of patients with mesothelioma may benefit from FGFR inhibition.



## Introduction

Malignant Pleural Mesothelioma (MPM) is a tumor arising from the pleural cavity and is strongly associated with occupational exposure to asbestos. Although strict regulation is in place in more than 50 countries, in parts of the world where there is still widespread usage of asbestos, most notably in South America, Russia and states of the former Soviet Republic, China and South-East Asia, the incidence of this disease is rising [1, 2]. MPM is highly refractory to conventional anticancer therapies, and the prognosis is poor; most patients die within a year of diagnosis. Surgery with curative intent is only possible in a highly selected group of patients and needs to be combined with chemotherapy. The only approved treatment, a combination of the cytotoxic agents cisplatin and pemetrexed, yields at best modest improvements in survival [3, 4]. Despite many clinical studies utilizing novel biological therapies, there are as yet no effective targeted therapies for this cancer [5, 6].

A recent comprehensive genomic analysis of 216 MPM samples found *BAP1, NF2, TP53, SETD2* and *CDKN2A* to be recurrently mutated or structurally rearranged [7]. The landscape is thus one of mutated tumor suppressor genes and alterations in pathways as diverse as Hippo, mTOR, and TP53, as well as histone methylation. Such loss-of-function oncogenic events are typically considered “undruggable”, but downstream programs of genes, activated as a consequence of such mutations, may themselves be tractable therapeutic targets. This is illustrated by NF2-deficient tumors with activated focal adhesion kinase (FAK). Defactinib, a FAK inhibitor, demonstrated efficacy in NF2-deficient tumors *in vitro* [8] but a subsequent clinical trial in mesothelioma was halted due to lack of efficacy. Other drugs tested to date that have failed to improve the outcome in MPM include EGFR inhibitors [9], Bcr-Abl inhibitors [10], thalidomide [11], bortezomib [12], and vorinostat [13]. In many of these studies, a subgroup of patients appeared to derive some benefit. However, in MPM, it has been difficult to elucidate reproducible biomarkers that identify these sensitive subgroups.

Some research groups have demonstrated coactivation of multiple RTK pathways in MPM tumors, which may provide a rationale for combination therapies with kinase inhibitors [14].

We aimed to utilize high-throughput chemical screening platforms alongside molecular characterization of immortalized and early-passage cell line models of MPM to uncover critical signaling pathways that may be amenable to therapeutic interrogation.

## Materials and methods

### Cell lines and tissue culture

Cells are grown and maintained in either RPMI or DMEM F/12 supplemented with 10% FBS and 1% penicillin/streptomycin. Cell lines were maintained at 37°C at 5% CO2. All cell lines have been verified by genotyping using short tandem repeat (STRs) profiling and Sequenom profiling of a panel of 92 single-nucleotide-polymorphisms.

### Cell viability Assays

Cells are trypsinized and counted before seeding at the optimal density for the well size (either 96- or 384-well plates were used) and duration of the assay. Seeding density was optimized by titration of the cells such that upon visual inspection of the control wells at the end of the assay, a confluency of 70% to 90% was observed allowing cells to grow in a linear phase. Adherent cell lines were seeded 24 hours before drug addition. The high-throughput chemical inhibitor screen was carried out using 384-well plates, and viability was measured 72 hours after drug addition with a 5-point serial fourfold concentration range of 265 compounds. All other viability assays were carried out using 96-well plates and a 9-point twofold dilution of the drugs. Drugs were all dissolved in DMSO, and DMSO was used only as a control condition. At the end of the experiment, cells were fixed with 4% paraformaldehyde. Following two washes with $dH_2O$, 100ml of Syto60 nucleic acid stain (Invitrogen) was added to a final concentration of 1mmol/L (a 1/5,000 stock dilution), and plates were fixed for 1hour at room temperature. Quantification of fluorescent signal was achieved using a Paradigm (BD) plate reader using excitation/emission wavelengths of 630/695 nm. Data were analyzed by adjusting for background signals and normalizing each well to the DMSO-treated control.

### High-throughput Screening Compounds

Compounds were acquired from academic collaborators or commercial vendors. Each compound, its therapeutically relevant target substrate and pathway, and the minimum and maximum screening concentrations are listed in Supplementary Table S1. Compounds were stored as 10 mmol/L aliquots at −80°C and were subjected to a maximum of 5 freeze-thaw

cycles. Each of the agents was screened at a 5-point serial fourfold dilution to provide a 256-fold range from the lowest to highest concentration. The concentrations selected for each compound were based on *in vitro* data to cover the range of concentrations known to inhibit relevant kinase activity and cell viability.

### Apoptosis assay

Cells were seeded in a flat-bottom 384 wells plate at optimal cell density. After 24 hours, PD173074 and AZD 4547 in a concentration range between 0.007813 and 1 µmol/L were added using a Tecan HP D300 Digital Dispenser. Five replicate wells were assayed for each condition. Phenylarsine oxide (20 µmol/L) was used as positive control condition. To assess apoptosis, 5 µmol/L of IncuCyte caspase-3/7 green apoptosis assay reagent was added to the cells. Confluence and apoptosis levels were quantified by IncuCyte Zoom live-cell imaging systems from Essen bioscience. Relative apoptosis was calculated by dividing the confluence of fluorescent apoptotic cells by total confluence and normalized to the positive control condition.



### Western Blots

Cell monolayers were lysed on ice in NP40 Cell Lysis Buffer (Invitrogen) containing fresh protease and phosphatase inhibitors (Roche). Lysates were centrifuged at 13,000 rpm for 10 minutes and the supernatant used for analyses. Protein concentration was calculated from a standard curve of BSA using the BCA assay (calbiotech) according to the manufacturer's instructions. Equal protein concentrations were loaded on pre-cast 4% to 12% Bis–Tris SDS-PAGE Gels (Invitrogen), run at 200 V for 1 hour. Proteins were transferred onto a methanol activated PVDF membrane at 100 V for 1 hour or overnight at 30 V. Membranes were blocked in 5% milk for 1 hour before the addition of primary antibody at a concentration recommended. After overnight incubation with the primary antibody at 4°C, the membrane was washed three times in 0.1% TBS-T followed by incubation with the secondary antibody according to suppliers description at 1/2,500 dilution). Immunoblots were imaged using Pierce Supersignal Plus chemiluminescent kit on a gel imager (Syngene). Antibodies against BAP1, pERK, ERK, pFGFR (total) and pFGFR1 (all from Cell Signalling Technologies) and the polyclonal p-FGFR3 antibody sc-33041 (Santa Cruz Biotechnology) were used. Beta Tubulin was used as a loading control for Western blots. Phospho-RTK arrays (RD systems) and caspase-Glo 3/7 assay were used according to the manufacturer's instructions.

### Establishment of early-passage primary mesothelioma tumor cell cultures

All patients whose materials were used provided written informed consent for the use and storage of pleural fluid, tumor biopsies and germ line DNA. Diagnosis was made on tumor biopsies according to local IHC protocols and confirmed by the Dutch Mesothelioma Panel, a national expert panel of certified pathologists that evaluate all suspected mesothelioma

patient samples. Early-passage primary mesothelioma cultures were generated from tumor cells isolated from pleural fluid of patients at the Netherlands Cancer Institute. The pleural fluid was centrifuged at 1,500 rpm for 5 minutes at room temperature. Erythrocyte lysis buffer was used to remove erythrocytes if many were present. Cells were resuspended in Dulbecco's Modified Eagle Medium (DMEM, Gibco) supplemented with peniciline/ streptomycin and 8% fetal calf serum. The cells were seeded in T75 flasks at a density of 1 x $10^6$ cells/mL and incubated at 37°C at a humidified 5% $CO_2$ atmosphere. Medium was refreshed depending on cell growth, usually twice a week. At seeding and during the first two passages, cytospins were made and stained with HE and reviewed by our pathologist to determine the percentage of tumor cells. If the tumor percentage was over 70%, usually reached after one passage, living cell cultures were transported to the Wellcome Trust Sanger Institute within 6 hours for drug screening and genetic analysis. Cells were cultured for a maximum period of 4 weeks.

### RNA interference and transfection

Lipofectamine RNAiMAX (Thermofisher) was used according to product guidelines for transfection with siRNA against FGFR3 (Thermo Fisher Silencer Select s5167 and s5169) or BAP1 (s15822) utilizing the protocol "forward transfection of mammalian cell lines". KIF11 siRNA (s7902) was used as a transfection (positive) control. Viability or protein expression were assayed as described above, at specified time points. H226 cell expressing a BAP1 stable construct, and BAP1 C91A mutant lines were a kind gift from K Kolluri (UCL, London).

### Gene expression analyses

Microarray data were generated on the Human Genome U219 96-Array Plate using the Gene Titan MC instrument (Affymetrix). The robust multi-array analysis (RMA) algorithm [15] was used to establish intensity values for each of 18562 loci (BrainArray v.10). We discarded transcripts with low sample variance and consolidated duplicated genes by averaging their expression values across duplicates. The resulting data were subsequently normalized ($\mu$=0; $\sigma$=1) sample-wise and gene-median centered. Raw data was deposited in ArrayExpress (accession: E-MTAB-3610). The RMA processed dataset is available at www.cancerrxgene.org/gdsc1000/GDSC1000_WebResources/Home.html. The expression-level signal of each gene was normalized using a nonparametric kernel estimation of its cumulative density function as described in ref.[16]. Additionally, the normalized expression values were further tissue-centered using as grouping factors the cell line tissue labels of ref. [17].

### MPM Mouse Xenograft Models

All animal experiments were conducted according to institutional guidelines under protocol approved by the animal ethics committee of the Netherlands Cancer Institute. To establish xenografts, 3 million human mesothelioma cells (H2731 and MSTO211H) were implanted

subcutaneously into the right dorsal flank of 6- to 7-week-old female nude SCID mice. Mice were randomized into vehicle and drugs treatment groups, and treatment was initiated once the tumor volumes reached approximately 200 $mm^3$. Tumor size was measured with calipers twice a week, and tumor volume was determined as $a \times b^2 \times 0.5$, where $a$ and $b$ were the large and small diameters, respectively.

## Results

### High-throughput chemical inhibitor screens in immortalized cell lines

A panel of 889 cancer cell lines was screened with 265 compounds that included targeted and cytotoxic compounds (for detail see http://www.cancerrxgene.org/). It was observed that three of 19 MPM lines (H2795, H2591, and MSTO-211H) had $IC_{50}$ values among the top 5% of cell lines showing highest sensitivity to the compound PD-173074, an FGFR1 and FGFR3 kinase inhibitor (Fig 1A; ref. 15). These three cell lines, together with two additional MPM lines (NCI-H28, resistant; MPP-89, partially sensitive) and an FGFR-dependent lung cancer cell line harboring amplification of FGFR1 (NCI-H1581), were rescreened with PD-173074 and were as sensitive to PD-173074 as the FGFR1-dependent lung cancer line NCI-1581 (Fig. 1B). Furthermore, this sensitivity was also seen with two more selective FGFR inhibitors, NVP-BGJ398 and AZD4547 (Supplementary Fig. S1). Sensitivity to PD-173074 in the MPM cell lines was confirmed by clonogenic survival assays (Fig. 1C). Although some sensitive lines died by apoptosis, as is shown by activated caspase activity with both PD-173074 and the multi-FGFR-targeted inhibitor AZD4547 (Fig. 1D and E), not all sensitive lines showed a dose incremental increase in this marker.

These data confirm previous findings [18] that a subset of MPM cell lines require FGF pathway activation for growth and survival, and that targeting this pathway could be a critical step in the control of these tumors.

### Drug sensitivity in early-passage MPM cultures

To test whether these observations could be reproduced in an independent cohort of primary mesothelioma cell lines, a panel of 11 pleural fluid-derived early-passage cultures from patients with MPM tumors were obtained and screened for viability using a panel of 48 small molecule inhibitors including PD-173074. Most of the early-passage cultures were resistant to virtually all agents (Supplementary Fig. S2). However, one MPM early-passage culture (NKI04) did demonstrate marked sensitivity to PD-173074. The sensitivity of NKI04 to FGFR inhibition was confirmed in a longer duration clonogenic survival assay, and the effect on cell viability was comparable to that seen in the FGFR1-amplified NCI-H1581 lung cancer cell line (Fig. 2A-C).

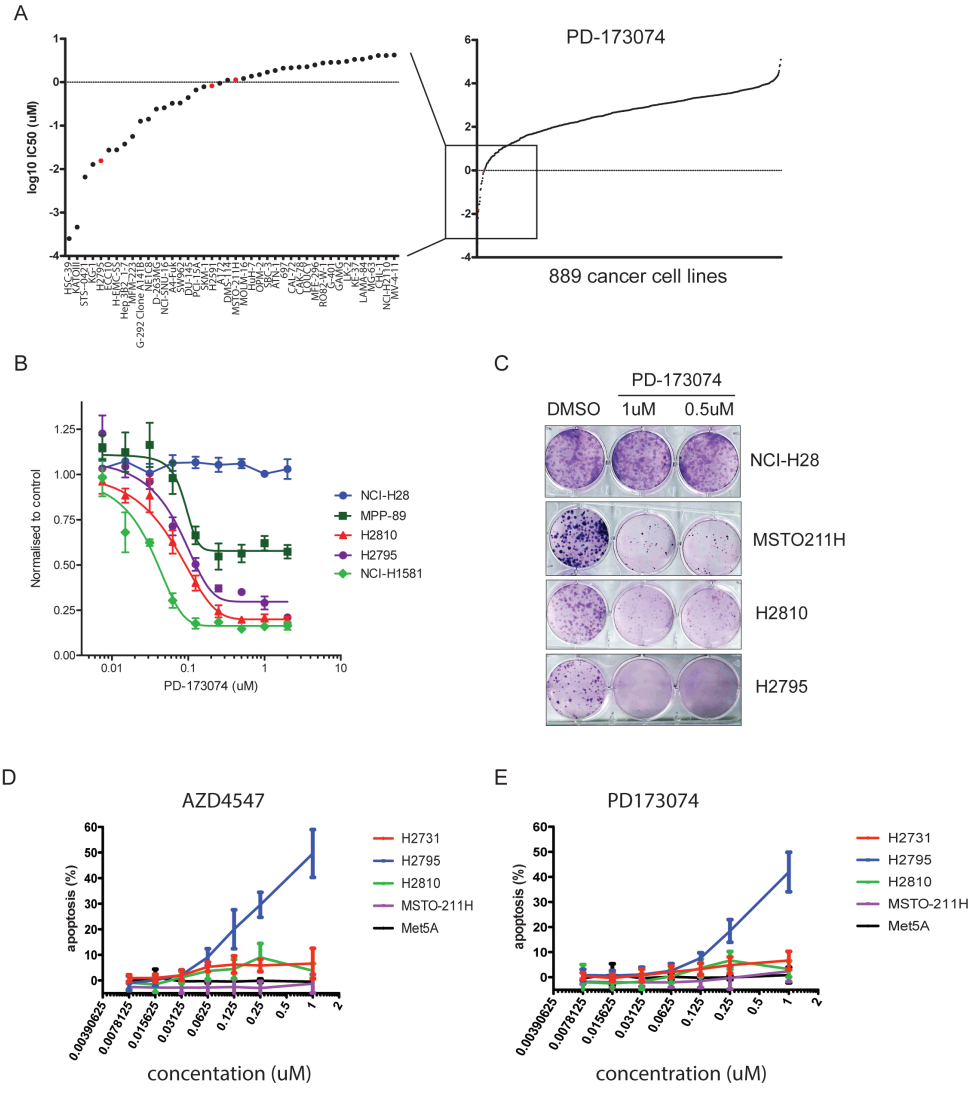


**Fig. 1. Sensitivity to FGFR inhibition in established mesothelioma cell lines. A)** Sensitivity to FGFR inhibitor PD173074 expressed as logIC50 value (inhibiting concentration that kills 50% of the cells) of each different cell line. The enlargement shows the 5% most sensitive cell lines with amongst them mesothelioma cell lines depicted in red. **B)** Dose–response curves depicting the cell viability (mean SD) of different cell lines (y-axis) as a function of the dose of FGFR inhibitor PD-173074. NCI-H28, MPP-89, H2810, and H2795 are mesothelioma cell lines, while NCI-H1581 is an FGFR-dependent lung cancer cell line. **C)** Fourteen-day clonogenic survival assay of selected mesothelioma cell lines (NCI-H28, MSTO-211H, H2810, and H2795), treated with FGFR inhibitor PD-173074 at concentrations of 500 nmol/L and 1 mmol/L. **D)** FGFR inhibitor AZD4547 kills mesothelioma cell lines via induction of apoptosis as is demonstrated by an increase in caspase 3/7 activity after 48 hours of treatment with different doses of AZD4547 in a panel of MPM cell lines. **E)** FGFR inhibitor PD173074 kills mesothelioma cell lines via induction of apoptosis as is demonstrated by an increase in caspase3/7 activity after 48 hours of treatment with different doses of PD-173074 a panel of MPM cell lines.

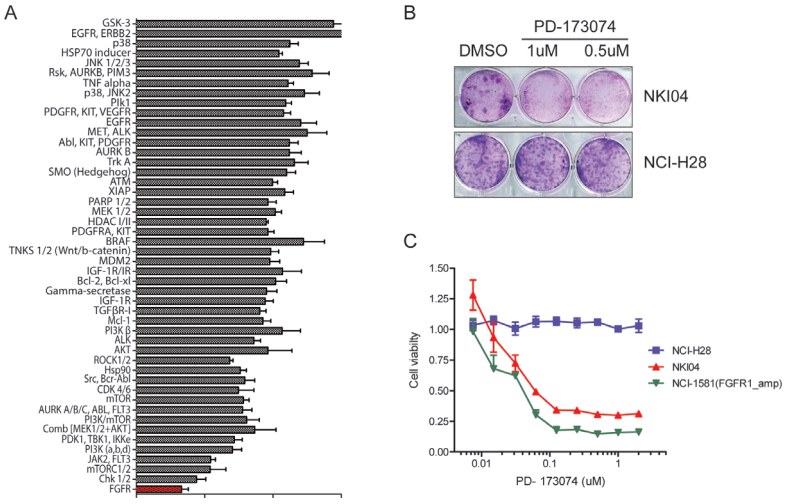


**Fig. 2. Sensitivity to FGFR inhibitors in primary mesothelioma lines. A)** Cell viability (mean SD) of primary mesothelioma line NKI04 after treatment with a fixed does of 48 different small molecule inhibitors. This cell line is most sensitive to FGFR inhibition. **B)** Fourteen-day clonogenic survival assay of primary mesothelioma line NKI04 compared with immortalized mesothelioma line NCI-H28 treated with FGFR inhibitor PD-173074 at concentrations of 500 nmol/L and 1 mmol/L.
**C)** Cell viability (mean SD) of primary mesothelioma line NKI04 compared with immortalized mesothelioma line NCI-H28 and FGFR-dependent lung cancer cell line NCI-H1581 (y-axis), as a function of the concentration of FGFR inhibitor PD-173074. NCI-H28, MPP-89, H2810, and H2795 are mesothelioma cell lines.



## Molecular characterization of FGF pathway signaling in cell lines and patient samples

In order to understand the basis for the observed sensitivity to FGFR inhibition, we analyzed whole-exome sequence and copy number array data for 21 MPM lines (http://cancer.sanger.ac.uk/cell_lines). There was no evidence of activating mutations or whole gene amplifications in any FGFR family member. RNA sequencing has been undertaken and shows no evidence of a fusion transcript involving any member of the FGFR family in any of the MPM cell lines (personal communication, M. Garnett). We then analyzed the corresponding gene expression data and focused on differential expression of FGFR and FGF family members in PD-173074-sensitive and -resistant MPM cell lines. Normalized expression of each of the FGF and FGFR family genes was correlated with sensitivity to PD-173074 to explore whether the variation in any single family member, either ligand or receptor, was associated with response to FGFR inhibition. We found a statistically significant correlation between elevated FGF9 mRNA expression and response to PD-173074 (P=0.0148) and AZD4547 treatment (P= 0.0098; Fig. 3A). FGF9 is a secreted, high-affinity ligand for the FGFR3 receptor, with low affinity for the FGFR1 and FGFR2 receptors [19]. To determine whether a subset of MPM exhibits elevated

expression of the FGF9 ligand in patients, we analyzed gene expression from a panel of 53 assorted MPM and matched normal lung clinical samples (Fig. 3B; ref. [20]). Overall, we observed significantly higher FGF9 transcript levels in MPM tumors compared with pleura and lung normal tissue ($P<0.0001$). Therefore, similar to our observation in the MPM cell lines, a subset of patient samples also demonstrates high levels of FGF9 expression.

### Modulation of FGF/FGFR function in MPM lines

A possible premise for the observed sensitivity of MPM lines that express high levels of FGF9 would be activation of the FGFR3 receptor kinase in an autocrine loop and subsequent engagement of prosurvival downstream signaling pathways. Indeed, a comparison of phosphorylation status of 42 receptor tyrosine kinases between a small sample of MPM cell lines demonstrated increased phosphorylation of FGFR3 in the sensitive line H2795 but not in resistant lines Met-5A and NCI-H28 (Fig. 3C).

To further confirm a critical role for FGFR3, this transcript was silenced by siRNA in a panel of MPM cell lines and the direct effect on cell viability was measured. Transient siRNA-mediated silencing of the FGFR3 transcript reduced cell viability in all 3 FGFR inhibitor-sensitive cell lines, but not in the FGFR inhibitor-resistant lines. This indicates a dependency on FGFR3 mediated signaling of the FGFR inhibitor-sensitive lines (Fig. 3D). As would be expected, inhibition of FGFR3 by the specific inhibitors AZD4547 and BJG398 decreased pERK levels (Fig. 3E), and this was also seen following siRNA-mediated silencing of FGFR3 in H2795 and MSTO-211H (Fig. 3F). The addition of FGF9 ligand to MPM cells lacking baseline FGFR3 activation was able to induce phosphorylation of FGFR3 and a change in the growth kinetics of this cell line in a dose-dependent fashion (Supplementary Fig. S5).

### Role of BAP1 in modulating FGF pathway signaling

Although we failed to identify genomic alterations in any member of the FGFR family that might explain the sensitivity to FGFR inhibition, we reasoned that this dependency might also be the consequence of other gene aberrations up- or downstream of FGFR3 signaling. We evaluated the gene expression and mutation database for other statistical associations explaining sensitivity to the FGFR inhibitor AZD4547 in the panel of MPM cell lines. We focused on driver mutations or copy-number alterations in three of the most frequently mutated genes in MPM, namely, *BAP1, NF2,* and *CDKN2A* [7]. We detected a weak but nonsignificant association between AZD4547 sensitivity and *BAP1* mutations in the sensitive cell lines (Fig. 4A). Given that loss of BAP1 protein expression might also occur through nonmutational mechanisms as previously described [21], we additionally characterized BAP1 protein status in these lines by Western blot analysis (Supplementary Figs. S3 and S4). When sensitivity to the AZD4547 was correlated with BAP1 protein expression (low/absent vs. expressed), there was a significant correlation between loss of BAP1 expression

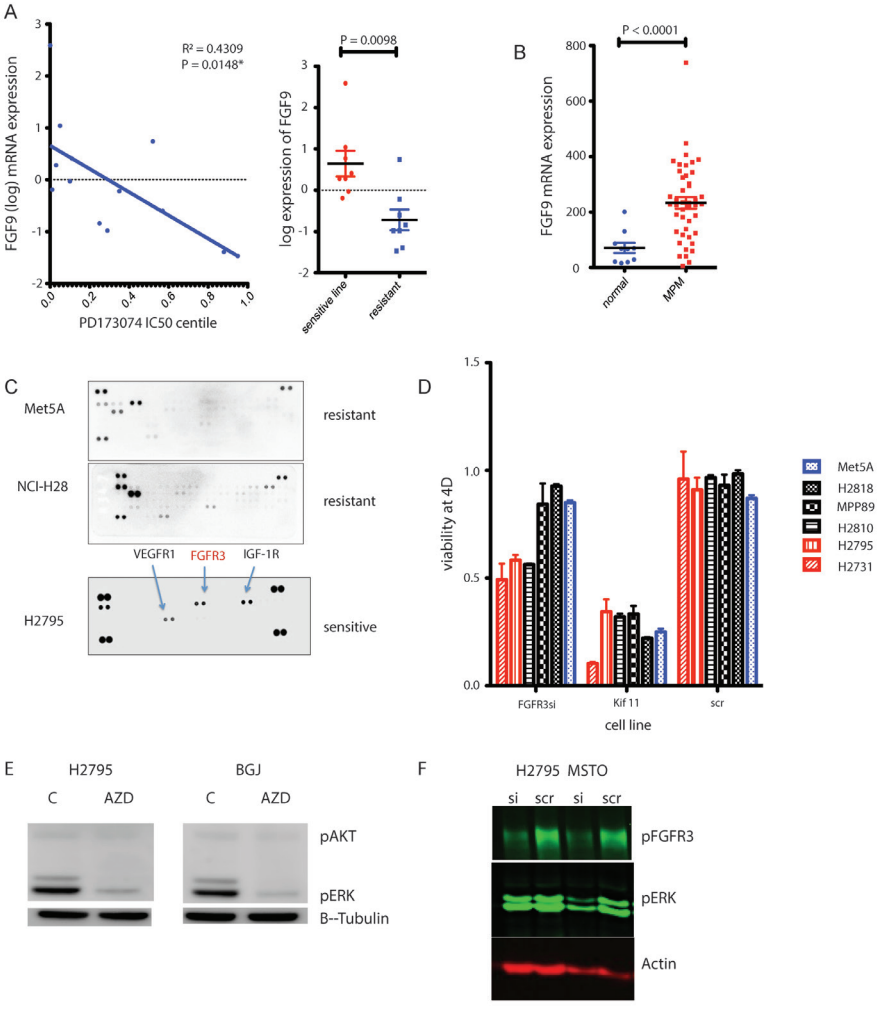


**Figure 3. FGFR inhibitor sensitivity is mediated by FGF axis signaling through FGF9 and FGFR3. A)** Scatterplot depicting sensitivity to FGFR inhibitor PD-173074 as a function of expression of FGF9. mRNA. Y-axis depicting log mRNA expression of FGF9 and x-axis showing centile of IC50 to PD173074 of individual MPM cell line in cell line screen. High FGF9 gene expression is significantly correlated to high sensitivity to FGFR inhibition. Right hand scatterplot showing FGF9 expression correlates with sensitivity to AZD4547. **B)** Expression of FGF9 in a set of MPM tumors, compared with normal lung and pleura, derived from GE0 dataset GSE2549. The mean expression in MPM tumors is significantly higher than that of normal lung and pleura. **C)** Phospho-RTK array reveals phosphorylated-FGFR3 in FGFR inhibitor–sensitive cell line H2795 that is absent in two resistant lines (NCI-H28 and Met5a). **D)** Cell viability of MPM cell lines after silencing of the FGFR3 transcript demonstrates reduced viability of FGFR inhibitor–sensitive cell lines H2795, H2810, and H2731 compared with FGFR inhibitor–resistant lines Met5A, NCI-H2052, H2810, and MPP89. Viability at 4 days post transfection is compared with Kif11–positive control siRNA and scrambled negative control. **E)** Modulation of pERK signaling in H2795 cell line following 6 hours of exposure to DMSO (C) or 500 nmol/L AZD4547 or DMSO and 100 nmol/L BGJ398. **F)** siRNA-mediated knockdown of pFGFR3 in H2795 and MSTO211H, showing effect on pFGFR3 and pERK versus scrambled control.

and sensitivity (P=0.0208; Fig. 4B).

### Functional consequences of BAP1 modulation on FGFR signaling.

Since silencing FGFR3 reduced cell viability in a subset of MPM lines, we next investigated whether this dependency on FGFR signalling was regulated by BAP1. BAP1 is a nuclear deubiquitinating enzyme with many unelucidated functions that might include modulation of the FGFR pathway. Silencing of BAP1 expression resulted in increased phosphorylation of FGFR3 (Figure 4C). Conversely, restoring BAP1 expression in the BAP1 null MPM line (Figure 4D) H226 resulted in a decrease in pFGFR and a modest increase in resistance to the FGFR inhibitor, AZD4547 (Figure 4E).

We observed increased expression at the protein level in the *BAP1* mutant cell lines of other RTK receptor genes and their appropriate ligands also known to be important in cell survival signaling in MPM such as PDGFRB, IGF1-R and MET [22] using phospho-RTK arrays (Supplementary Fig. S4A and S4B). The H226-null MPM cell line was transfected with a wild-type BAP1 construct and a functionally inactive C91A-mutant BAP1 construct. Gene expression analysis on these two lines was performed and Signaling Pathway Impact Analysis (SPIA) of the data (Supplementary Table S) demonstrated that among the most significantly activated pathways in BAP1-inactive cells is the “Bladder Cancer” pathway including FGFR3 (arrow, Supplementary Fig. S6A) illustrated in Supplementary Figure S6B [23]. In summary, the gene expression analysis demonstrates that BAP1 loss of function is associated with a transcriptional response upregulating not only FGFR signaling but also other RTKs such as PDGFRB, CMET and IGF1R, that may be important mediators of cell growth and survival. However, only FGFR inhibitors showed a significant viability effect as single agents. We analyzed gene expression data from a study of 51 mesothelioma tumor samples to see if a similar effect on the FGFR pathway was seen *in vivo* (40 *BAP1* wild-type and 11 mutant; GEO GSE29354; ref. [24]). Amongst members of the FGFR signaling family, *BAP1*-mutant tumors did indeed demonstrate increased expression of FGF18, FGFR2, and FGFR3 relative to *BAP1* wild-type tumors (Supplementary Table). To explore this association further in human tumors, we analyzed the available TCGA data and looked for the incidence of genetic and mRNA alterations of these genes in MPM tumors by *BAP1* status (Fig. 4F). This showed the majority of dysregulation (10 of 14) events in FGF9, FGF18, and FGFR3 occurred in the context of BAP1 gene of mRNA dysregulation.

### FGFR inhibition in MPM xenograft model

To assess the *in vivo* efficacy of targeting FGFR in MPM, we established a xenograft model using the FGFR inhibitor-sensitive MPM lines H2795 and MSTO-211H. Mice were treated with AZD4547, a selective inhibitor of FGFR1/2/3, which is currently being evaluated in clinical trials. We observed that treatment with AZD4547 resulted in significant growth

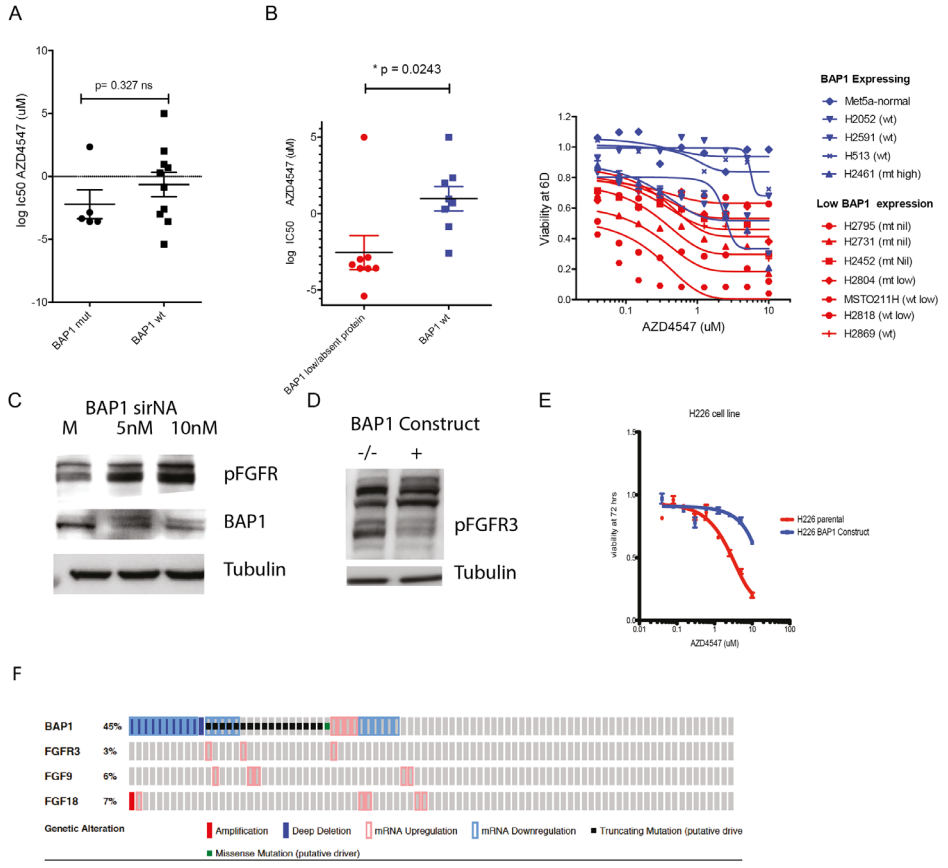


**Figure 4. Loss of BAP1 protein expression is correlated to FGFR inhibitor sensitivity. A)** Sensitivity to FGFR inhibitor AZD4547—expressed as log$IC_{50}$ value—of cell lines, grouped according to BAP1 mutation status. The mean log$IC_{50}$ value is not significantly different between the two groups. **B)** Sensitivity to FGFR inhibitor AZD4547 according to BAP1 protein expression. Red are cell lines with low or absent BAP1 protein. Blue lines have normal BAP1 protein expression. Sensitivity (left) is expressed as log$IC_{50}$ value (y-axis). The difference between the two groups is statistically significant. Cell viability (right) of different mesothelioma lines (y-axis) after treatment with FGFR inhibitor AZD4547 (x-axis). wt, wild-type; mt, mutant; high, high protein expression; low, low protein expression; nil, no protein expression. Right-hand panel showing dose–response curves of MPM cell lines treated with FGFR inhibitor AZD4547. Cell lines in red are lines with low or absent BAP1 protein expression. Blue lines have normal BAP1 protein expression. **C)** SiRNA-mediated depletion of BAP1 in H2052 at increasing siRNA doses of 5 and 10 nmol/L versus mock transfected (M) control. Western blot comparing pFGFR3 and BAP1 expression at these conditions. Tubulin as loading control. **D)** BAP1 overexpression in BAP1-null cell line H226. Western blot of BAP1 construct versus parental cell line baseline pFGFR levels with tubulin as loading control. **E)** Cell viability after treatment with increasing doses of FGFR inhibitor AZD4547 in parental cell line H226 BAP1-null (red) and in the same cell line with BAP1 construct (red). BAP1 overexpression increases cell viability after FGFR inhibition. **F)** Co-occurence of somatic mutations in BAP1 and FGFR family members in MPM tumors in the TCGA cohort.

inhibition in the H2795- and MSTO-211H-derived tumors (Fig. 5A). Furthermore, AZD45457 treated tumors showed a reduction in pERK signaling by immunohistochemistry compared with vehicle control-treated tumors (Fig. 5B), indicating target engagement by the drug in this model. Caspase activation was also seen in drug-treated tumors suggesting apoptosis (Supplementary Fig. S7).

## Combination therapeutic screen

As the single-agent efficacy of FGFR inhibition was seen only in a subset of MPM cell lines, and because persistent pAKT pathway activation was seen in cell lines not responsive to FGFR inhibition, we hypothesized that a combination screen utilizing a PI3 kinase inhibitor may reveal useful synergies. We undertook an anchor-based combination screen in 15 MPM

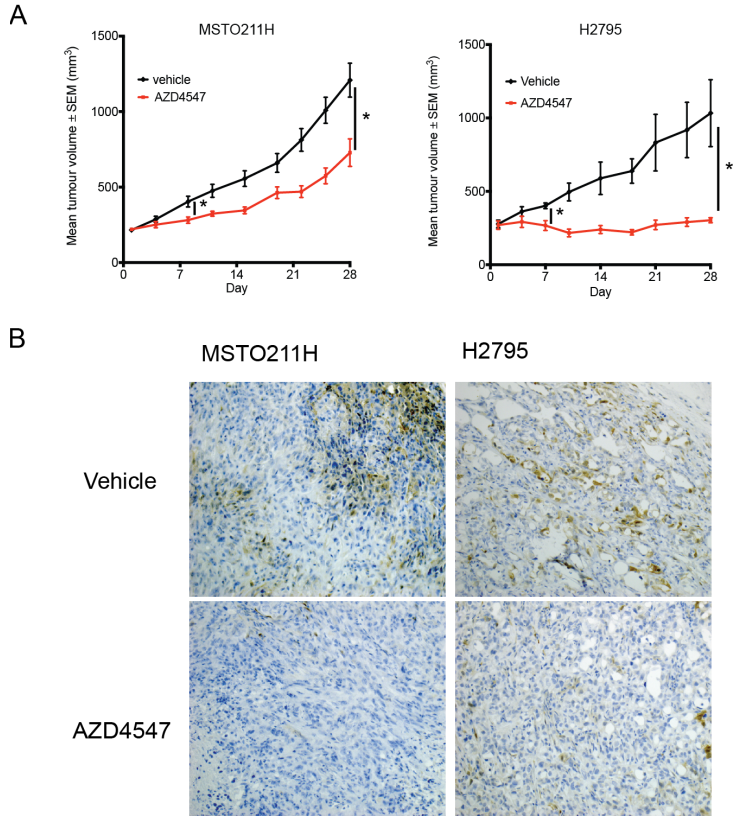


**Figure 5. Xenograft mouse model shows FGFR inhibition efficacy in vivo. A)** Xenograft mouse model using mesothelioma cell lines H2795 and MSTO211H. Mean tumor volume is depicted on the y-axis as a function of time (x-axis). Red lines indicate tumor growth in mice treated with FGFR inhibitor AZD4547, while the black lines indicate growth in vehicle-treated mice. **B)** Immunohistochemistry of AZD4547-versus vehicle control-treated xenograft tumors. ppERK expression in representative tumors in drug-treated versus vehicle control groups.

cell lines using 95 small-molecule inhibitors (see supplementary Table for details) selected to target many critical pathways in cancer, both as single agents and in combination with a fixed dose of the PI3 Kinase inhibitor AZD6482. The resulting difference in area under the curve (AUC) between single agent small-molecule inhibitor and the combination with AZD6482 was used to calculate synergy. The most recurrent synergistic interactions were seen with IGF1R inhibitor BMS-536924 and FGFR inhibitor PD-173074 (Supplementary Fig. S8A) with synergy observed in seven and six of 15 lines, respectively. Supplementary Fig. S8B shows a validation dose-response curve of the FGFRi-resistant NCI-H28 cell line showing minimal effect of BMS-536824 or AZD6482 alone, but reduced viability and pAKT reduction with the combination. This cytotoxicity is not seen in the mesothelial control cell line Met5a, suggesting that the synergy is not generic but cell line specific.

## Discussion

Because MPM is a rare and heterogeneous tumor, it is notoriously difficult to identify and characterize responding subgroups in clinical trials. Our work illustrates the application and possibilities of comprehensive pharmacogenomic profiling approaches in intractable cancers such as MPM. The finding of FGFR inhibitor sensitivity in a subgroup of immortalized MPM cell lines represents a potentially novel therapeutic approach for this tumor type. As immortalized cell lines may undergo genetic drift, we also confirmed our findings in primary mesothelioma early-passage lines.

Dysregulation of the FGFR pathway has been described in many cancer types [25, 26]. FGF9 signaling through FGFR3 has been shown to have a role in the development and progression of tumor cells in mouse models for NSCLC and prostate cancer [27]. In MPM cell line models, we observed that high levels of the ligand FGF9 were strongly correlated with sensitivity to the FGFR inhibitors PD-173074 and AZD4547. We hypothesize that the effects of FGF9 are mediated through FGFR3 signaling, as illustrated by modulation of downstream ERK phosphorylation upon chemical inhibition with small-molecule inhibitors of FGFR3 and knockdown of FGFR3. FGFR3 is conversely not phosphorylated in cell lines insensitive to FGFRi, and this phosphorylation can be induced by the addition of synthetic FGF9 ligand. Interestingly, there was variability in FGF9 mRNA expression levels among the MPM cell lines, similar to what is observed in tumors in previously published studies. Recently, other groups demonstrated efficacy of FGFR inhibition in preclinical models of MPM mediated by other FGF-pathway members such as FGFR1 [18, 28, 29]. We confirm the efficacy of a clinically utilized FGFR inhibitors including AZD4547 *in vivo* in MPM xenograft models. Furthermore, since undertaking these studies, early-phase clinical work with pharmacokinetic data has been published [30, 31] on AZD4547 and BGJ398. These have confirmed that the doses used in the *in vitro* work (100 nmol/L to µmol/L) here are achievable in plasma *in vivo* and are

able to modulate the target, with pharmacodynamic end points of target engagement with FRS2 downregulation and changes in serum phosphate levels seen.

FGF receptors and ligands are being targeted in clinical trials by both selective and nonselective FGFR TKI's and monoclonal antibodies [32] and AZD4547 has shown modest clinical activity in tumors with FGFR pathway aberrant activation [33]. In MPM dovitinib, a multitargeting kinase inhibitor with activity against FGFR has been trialed and has failed in small cohort of patients with MPM [34]. Because the data across tumor types demonstrate only a small group of patients responds to FGFR inhibition, it is crucial to find biomarkers that predict response to FGFR inhibition. Guagnano et al. integrated genomic and transcriptomic data of about 500 tumor cell lines with drug-sensitivity data to find predictive biomarkers for response to FGFR inhibitor NVP-BGJ398. A genetic alteration in one of the four FGF receptors was found in 7% of cell lines, but only about half of the cell lines with such an alteration was found to be sensitive [35].

We did not find any mutation, amplification, or fusion transcripts of the FGFR family in the inhibitor-sensitive MPM cell lines. The genes that were most recurrently altered in our MPM cell lines include *CDKN2A, BAP1* and *NF2.* The frequency at which these genes were mutated is broadly similar to those previously described in clinical MPM samples [6, 7].

We show that loss of BAP1 expression was associated with sensitivity to FGFR inhibition. This finding was further validated with modulation of pFGFR signaling and dose-response kinetics to FGFR inhibition following siRNA-mediated knockdown and BAP1 overexpression in MPM cell lines. Caveats with this association were also observed: NCI-H28 was one of the most resistant cell lines to FGFR inhibition but carried a *BAP1* homozygous deletion, suggesting that BAP1 loss may enrich for FGFR inhibitor-sensitive cell lines but that some heterogeneity of drug response may still be observed. BAP1 (BRCA-associated protein 1) is a nuclear deubiquinating enzyme that controls gene expression by interaction with numerous transcription factors and other complexes, including those of the double strand DNA-break repair machinery [36]. BAP1 thus influences cell-cycle progression [37] and double-strand DNA break repair [38]. We show here that its loss may also affect gene expression of FGF pathway members, thereby enhancing signaling through this pathway.

The *BAP1* gene is inactivated by somatic mutation in 23% to 64% of patients with MPM and between 1% to 47% in other tumor types [24, 39-43]. Furthermore, BAP1 protein levels are undetectable in about 25% of MPM with normal *BAP1* gene status, likely by epigenetic modification [24]. BAP1 loss was observed to enrich for FGFR inhibitor-sensitive MPM lines, and expression of C91 hydrolase inactive mutant versus wild-type BAP1 protein in the H226 cell line induced activation of FGFR3 signaling. We hypothesized that inactivation of BAP1

in MPM, possibly through its function as a ubiquitin hydrolase, induces changes in gene expression of both FGF family ligands and receptors to stimulate cell growth and survival.

We performed a combination drug screen to assess the impact of novel combinations of targeted therapies on MPM cell lines. On the 15 MPM cell lines screened, we found that FGFR and IGF1R inhibitors were the most recurrently synergistic with the PI3-kinase inhibitor AZD6482. This is the first time, to our knowledge, that both a single agent and combination therapeutic screen have been performed, which point to the primacy of the FGFR signaling pathway in MPM. Interestingly, one of the most resistant cell lines to FGFR inhibition was amenable to treatment with AZD6482 plus IGF1R inhibition with evidence of ablation of pAKT with the combination of drugs but not with either alone, implying true synergy. Previous studies have identified that multiple RTK's are active in MPM [14], and this has provided some rationale to consider combination therapies to overcome innate resistance to targeted therapies. It is also interesting to speculate as to whether IGF1R plus PI3K inhibition would be of use in acquired resistance to FGFR inhibitors.



## Conclusion

High-throughput drug screening revealed a subset of both immortalized and primary mesothelioma cell lines to be highly sensitive to FGFR-inhibition. This sensitivity was mediated through FGFR3 and was associated with loss of BAP1 protein expression. The high incidence of BAP1 protein loss in MPM tumors implies potential benefit from FGFR inhibition for a substantial subset of this patient group. In addition, our anchor-based screens revealed synergistic combinations that helped to overcome innate resistance to FGFR inhibition.

## References


1. van Meerbeeck, J.P., et al., *Malignant pleural mesothelioma: the standard of care and challenges for future management.* Crit Rev Oncol Hematol, 2011. **78**(2): p. 92-111.
2. Frank, A.L. and T.K. Joshi, *The global spread of asbestos.* Ann Glob Health, 2014. **80**(4): p. 257-62.
3. Baas, P., et al., *Malignant pleural mesothelioma: ESMO Clinical Practice Guidelines for diagnosis, treatment and follow-up.* Ann Oncol, 2015. **26 Suppl 5**: p. v31-9.
4. Vogelzang, N.J., et al., *Phase III study of pemetrexed in combination with cisplatin versus cisplatin alone in patients with malignant pleural mesothelioma.* J Clin Oncol, 2003. **21**(14): p. 2636-44.
5. Pinton, G., et al., *Therapies currently in Phase II trials for malignant pleural mesothelioma.* Expert Opin Investig Drugs, 2013. **22**(10): p. 1255-63.
6. Ladanyi, M., et al., *New strategies in pleural mesothelioma: BAP1 and NF2 as novel targets for therapeutic development and risk assessment.* Clin Cancer Res, 2012. **18**(17): p. 4485-90.
7. Bueno, R., et al., *Comprehensive genomic analysis of malignant pleural mesothelioma identifies recurrent mutations, gene fusions and splicing alterations.* Nat Genet, 2016. **48**(4): p. 407-16.
8. Shapiro, I.M., et al., *Merlin deficiency predicts FAK inhibitor sensitivity: a synthetic lethal relationship.* Sci Transl Med, 2014. **6**(237): p. 237ra68.
9. Govindan, R., et al., *Gefitinib in patients with malignant mesothelioma: a phase II study by the Cancer and Leukemia Group B.* Clin Cancer Res, 2005. **11**(6): p. 2300-4.
10. Mathy, A., et al., *Limited efficacy of imatinib mesylate in malignant mesothelioma: a phase II trial.* Lung Cancer, 2005. **50**(1): p. 83-6.
11. Baas, P., et al., *Thalidomide in patients with malignant pleural mesothelioma.* Lung Cancer, 2005. **48**(2): p. 291-6.
12. Fennell, D.A., et al., *Phase II clinical trial of first or second-line treatment with bortezomib in patients with malignant pleural mesothelioma.* J Thorac Oncol, 2012. **7**(9): p. 1466-70.
13. Krug, L.M., et al., *Vorinostat in patients with advanced malignant pleural mesothelioma who have progressed on previous chemotherapy (VANTAGE-014): a phase 3, double-blind, randomised, placebo-controlled trial.* Lancet Oncol, 2015. **16**(4): p. 447-56.
14. Menges, C.W., et al., *A Phosphotyrosine Proteomic Screen Identifies Multiple Tyrosine Kinase Signaling Pathways Aberrantly Activated in Malignant Mesothelioma.* Genes Cancer, 2010. **1**(5): p. 493-505.
15. Irizarry, R.A., et al., *Exploration, normalization, and summaries of high density oligonucleotide array probe level data.* Biostatistics, 2003. **4**(2): p. 249-64.
16. Hanzelmann, S., R. Castelo, and J. Guinney, *GSVA: gene set variation analysis for microarray and RNA-seq data.* BMC Bioinformatics, 2013. **14**: p. 7.
17. Iorio, F., et al., *A Landscape of Pharmacogenomic Interactions in Cancer.* Cell, 2016. **166**(3): p. 740-754.
18. Marek, L.A., et al., *Nonamplified FGFR1 is a growth driver in malignant pleural mesothelioma.* Mol Cancer Res, 2014. **12**(10): p. 1460-9.
19. Zhang, X., et al., *Receptor specificity of the fibroblast growth factor family. The complete mammalian FGF family.* J Biol Chem, 2006. **281**(23): p. 15694-700.
20. Gordon, G.J., et al., *Identification of novel candidate oncogenes and tumor suppressors in malignant pleural mesothelioma using large-scale transcriptional profiling.* Am J Pathol, 2005. **166**(6): p. 1827-40.
21. Shah, A.A., T.D. Bourne, and R. Murali, *BAP1 protein loss by immunohistochemistry: a potentially useful tool for prognostic prediction in patients with uveal melanoma.* Pathology, 2013. **45**(7): p. 651-6.
22. Brevet, M., et al., *Coactivation of receptor tyrosine kinases in malignant mesothelioma as a rationale for combination targeted therapy.* J Thorac Oncol, 2011. **6**(5): p. 864-74.
23. Tarca, A.L., et al., *A novel signaling pathway impact analysis.* Bioinformatics, 2009. **25**(1): p. 75-82.
24. Bott, M., et al., *The nuclear deubiquitinase BAP1 is commonly inactivated by somatic mutations and 3p21.1 losses in malignant pleural mesothelioma.* Nat Genet, 2011. **43**(7): p. 668-72.
25. Dienstmann, R., et al., *Genomic aberrations in the FGFR pathway: opportunities for targeted therapies in solid tumors.* Ann Oncol, 2014. **25**(3): p. 552-63.
26. Helsten, T., et al., *The FGFR Landscape in Cancer: Analysis of 4,853 Tumors by Next-Generation Sequencing.* Clin Cancer Res, 2016. **22**(1): p. 259-67.
27. Suzuki, T., et al., *Multiple roles of extracellular fibroblast growth factors in lung cancer cells.* Int J Oncol, 2015. **46**(1): p. 423-9.
28. Schelch, K., et al., *Fibroblast growth factor receptor inhibition is active against mesothelioma and synergizes with radio- and chemotherapy.* Am J Respir Crit Care Med, 2014. **190**(7): p. 763-72.

29. Plones, T., et al., *Absence of amplification of the FGFR1-gene in human malignant mesothelioma of the pleura: a pilot study.* BMC Res Notes, 2014. **7**: p. 549.
30. Nogova, L., et al., *Evaluation of BGJ398, a Fibroblast Growth Factor Receptor 1-3 Kinase Inhibitor, in Patients With Advanced Solid Tumors Harboring Genetic Alterations in Fibroblast Growth Factor Receptors: Results of a Global Phase I, Dose-Escalation and Dose-Expansion Study.* J Clin Oncol, 2017. **35**(2): p. 157-165.
31. Gavine, P.R., et al., *AZD4547: an orally bioavailable, potent, and selective inhibitor of the fibroblast growth factor receptor tyrosine kinase family.* Cancer Res, 2012. **72**(8): p. 2045-56.
32. Touat, M., et al., *Targeting FGFR Signaling in Cancer.* Clin Cancer Res, 2015. **21**(12): p. 2684-94.
33. Paik, P.K., et al., *A Phase Ib Open-Label Multicenter Study of AZD4547 in Patients with Advanced Squamous Cell Lung Cancers.* Clin Cancer Res, 2017. **23**(18): p. 5366-5373.
34. Laurie, S.A., et al., *A phase II trial of dovitinib in previously-treated advanced pleural mesothelioma: The Ontario Clinical Oncology Group.* Lung Cancer, 2017. **104**: p. 65-69.
35. Guagnano, V., et al., *FGFR genetic alterations predict for sensitivity to NVP-BGJ398, a selective pan-FGFR inhibitor.* Cancer Discov, 2012. **2**(12): p. 1118-33.
36. Yu, H., et al., *The ubiquitin carboxyl hydrolase BAP1 forms a ternary complex with YY1 and HCF-1 and is a critical regulator of gene expression.* Mol Cell Biol, 2010. **30**(21): p. 5071-85.
37. Eletr, Z.M. and K.D. Wilkinson, *An emerging model for BAP1's role in regulating cell cycle progression.* Cell Biochem Biophys, 2011. **60**(1-2): p. 3-11.
38. Yu, H., et al., *Tumor suppressor and deubiquitinase BAP1 promotes DNA double-strand break repair.* Proc Natl Acad Sci U S A, 2014. **111**(1): p. 285-90.
39. Yoshikawa, Y., et al., *Frequent inactivation of the BAP1 gene in epithelioid-type malignant mesothelioma.* Cancer Sci, 2012. **103**(5): p. 868-74.
40. Nasu, M., et al., *High Incidence of Somatic BAP1 alterations in sporadic malignant mesothelioma.* J Thorac Oncol, 2015. **10**(4): p. 565-76.
41. Murali, R., T. Wiesner, and R.A. Scolyer, *Tumours associated with BAP1 mutations.* Pathology, 2013. **45**(2): p. 116-26.
42. Lu, C., et al., *The genomic landscape of childhood and adolescent melanoma.* J Invest Dermatol, 2015. **135**(3): p. 816-23.
43. Carbone, M., et al., *Combined Genetic and Genealogic Studies Uncover a Large BAP1 Cancer Syndrome Kindred Tracing Back Nine Generations to a Common Ancestor from the 1700s.* PLoS Genet, 2015. **11**(12): p. e1005633.

## Supplementary figures and tables

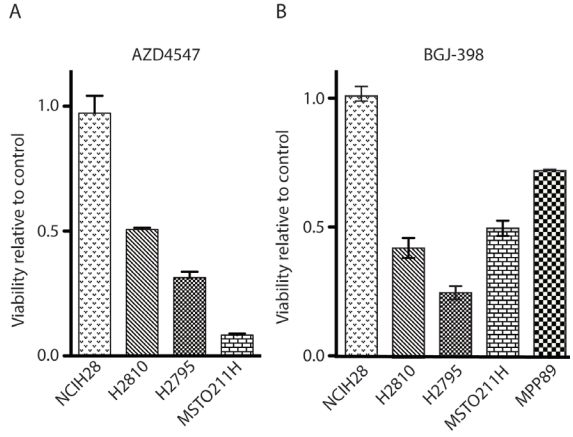


**Fig. S1. A subset of MPM cell lines respond to FGFR inhibition.** Cell viability of selected mesothelioma cell lines (NCI-H28, H2810, H2795, MSTO-211H and MPP-89) after 72 hours of treatment with **A)** AZD4547 at a fixed dose of 500 nmol/L and **B)** BGJ398 at a fixed dose of 300 nmol/L

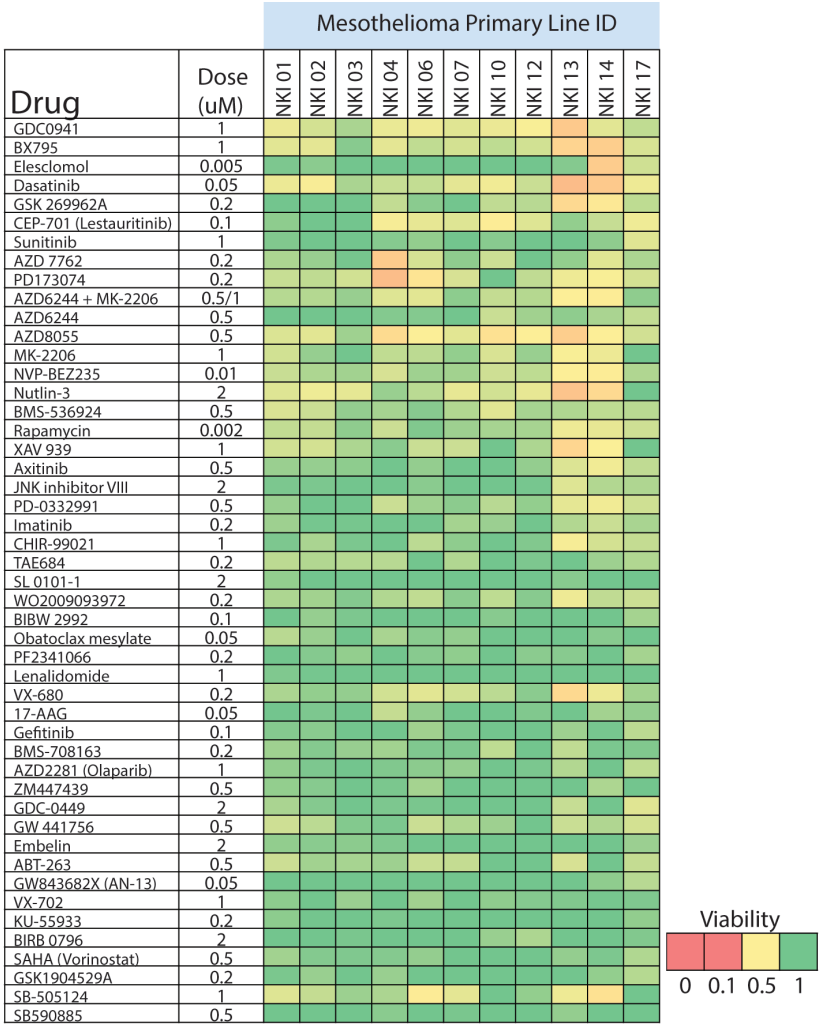


**Fig. S2. A subset of pleural fluid derived early passage primary cultures (EPL) respond to FGFR inhibition.** Cell viability of 11 early passage primary cultures (columns) after treatment with a fixed dose of 48 small molecular inhibitors (rows), depicted in a color scale (green: 100% cell viability; red: 0% cell viability).

A

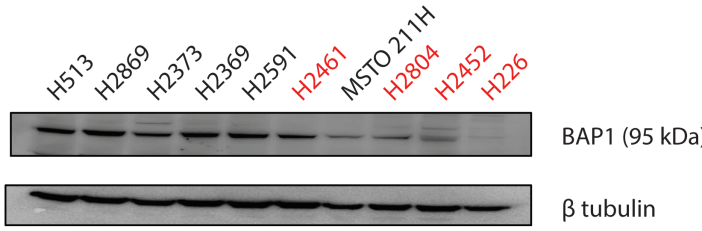


B

| Cell line | CHR | GENE_NAME | CDS_SYNTAX | AA_MUT_SYN | Class | DESCRIPTION |
|---|---|---|---|---|---|---|
| H2461 | 3 | BAP1 | c.65delT | p.F22fs*50 | indel | Deletion - Frameshift |
| H2722 | 3 | BAP1 | c.? | p.0 | indel | HomDel |
| H2731 | 3 | BAP1 | c.123-15_131( | p.? | indel | Essential Splice |
| H2795 | 3 | BAP1 | c.38-7_49del1 | p.? | indel | Essential Splice |
| H2804 | 3 | BAP1 | c.37+4_37+5in | p.? | indel | Essential Splice |
| IST-MES1 | 3 | BAP1 | c.1983+1_198 | p.? | indel | Essential Splice |
| NCI-H2452 | 3 | BAP1 | c.284C>A | p.A95D | Missense | Substitution - Missense |
| NCI-H28 | 3 | BAP1 | c.438-19_441( | p.? | indel | Essential Splice |

**Fig. S3. BAP1 mutation status does not correlate fully with protein expression. A)** Werstern Blot showing BAP1 protein expression in several MPM cell lines, both BAP1 wild type (black) and mutant lines (red). Beta tubulin represents the proetin loading control. **B)** List of somatic mutations in BAP1 seen in MPM cell lines

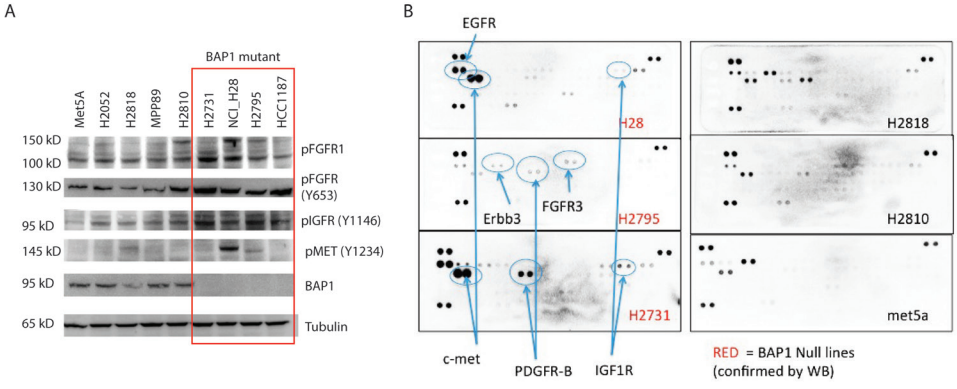


**Fig. S4. BAP1 null cell lines show increased activity of multiple tyrosine kinases. A)** Western Blot showing BAP1 protein expression in several MPM cell lines as well as activation in IGFR, MET, and FGFR. **B)** Phospho RTK array panel showing baseline RTK activation of BAP1 mutant (highlighted in red) versus wild type mesotheliomas.

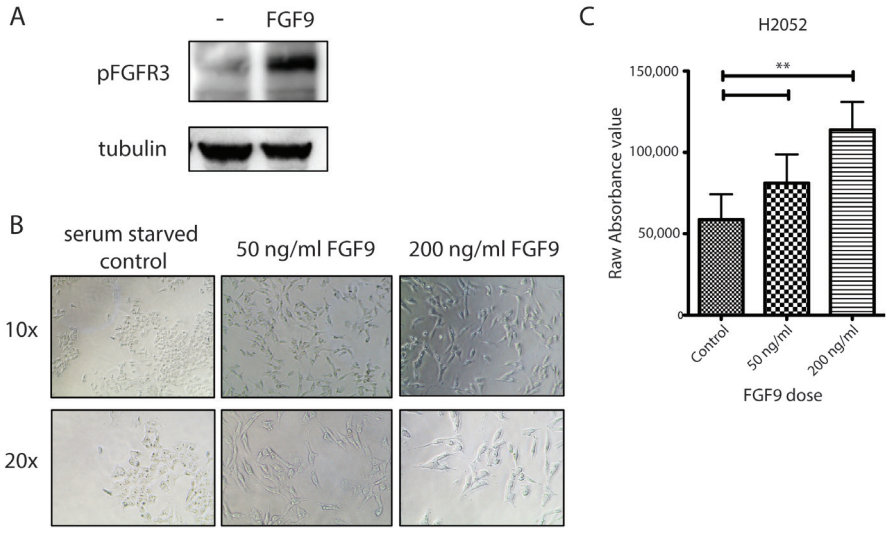


**Fig. S5. FGF 9 activated FGFR3 modulated growth and phenotype. A)** Western Blot of pFGFR in serum starved H2052 MPM cell line at baseline and with the addition of 50 ng/mL of recombinant FGF9 ligand after 1 hour. **B)** Light microscopy of H2052 cell line under serum starved conditions, and with the addition of FGF9 ligand at varying concentrations. **C)** Comparative viability of H2052 by syto 60 assay at baseline and following the addition of 50 ng/mL and 200 ng/mL FGF9 ligand.

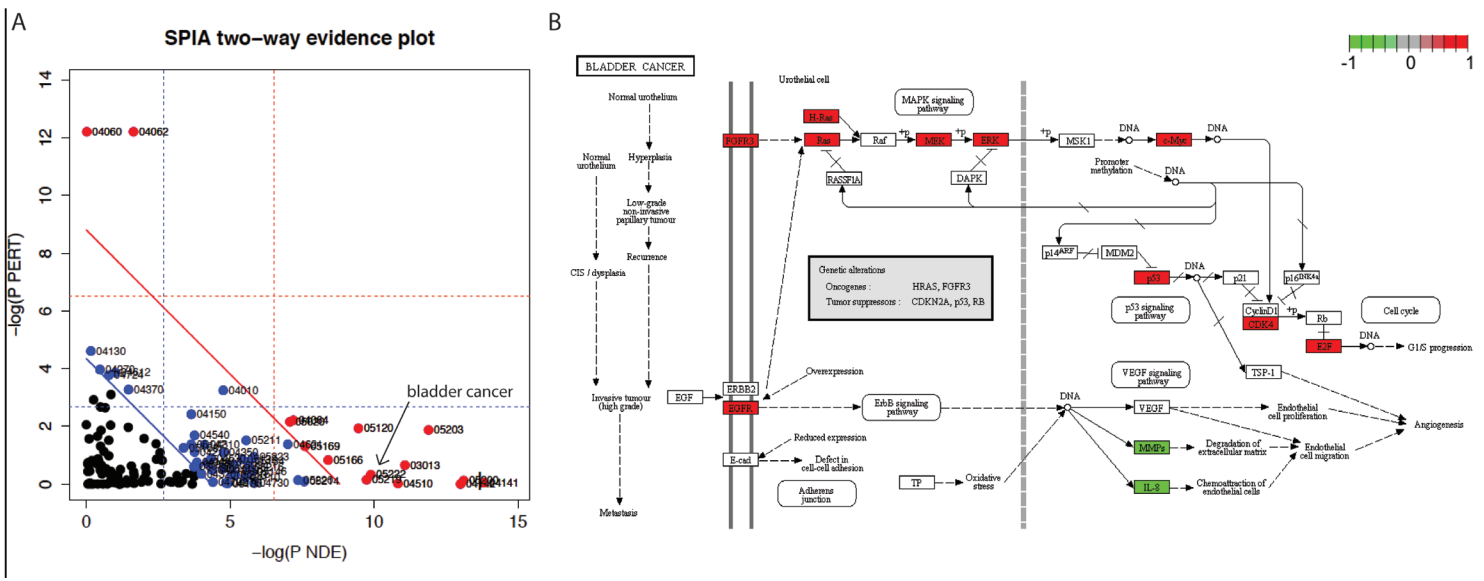


**Fig. S6. BAP1 modulation and FGFR pathway activation by gene expression.** (A) Gene expresssion analysis of H226 cell line (BAP1 null) transfected with wild type BAP1 construct vs BAP1 inactive (c91a) construct. SPIA pathway analysis of C91A vs wild type cell line revealed the KEGG “bladder cancer”pathway is significant acivated in C91A cell line arrow. (B) Bladder cancer pathway showing overexpressed genes in C91A line in red.

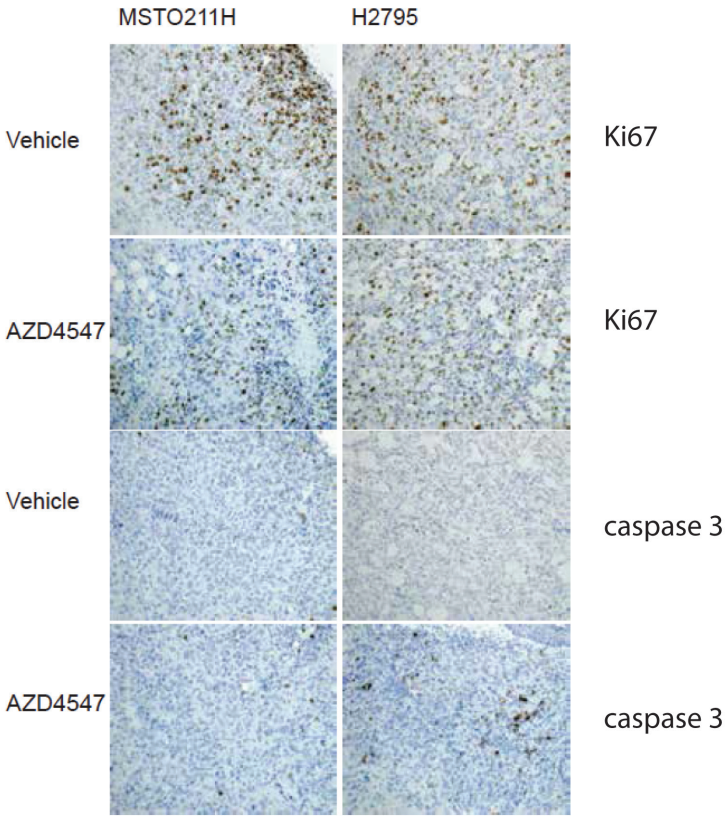


**Fig. S7. Xenograft tumor immunohistochemistry.** Immunohistochemistry for Caspase 3 and Ki67 in MPM xenograft tumors during vehicle control adn AZD4547 treated conditions.

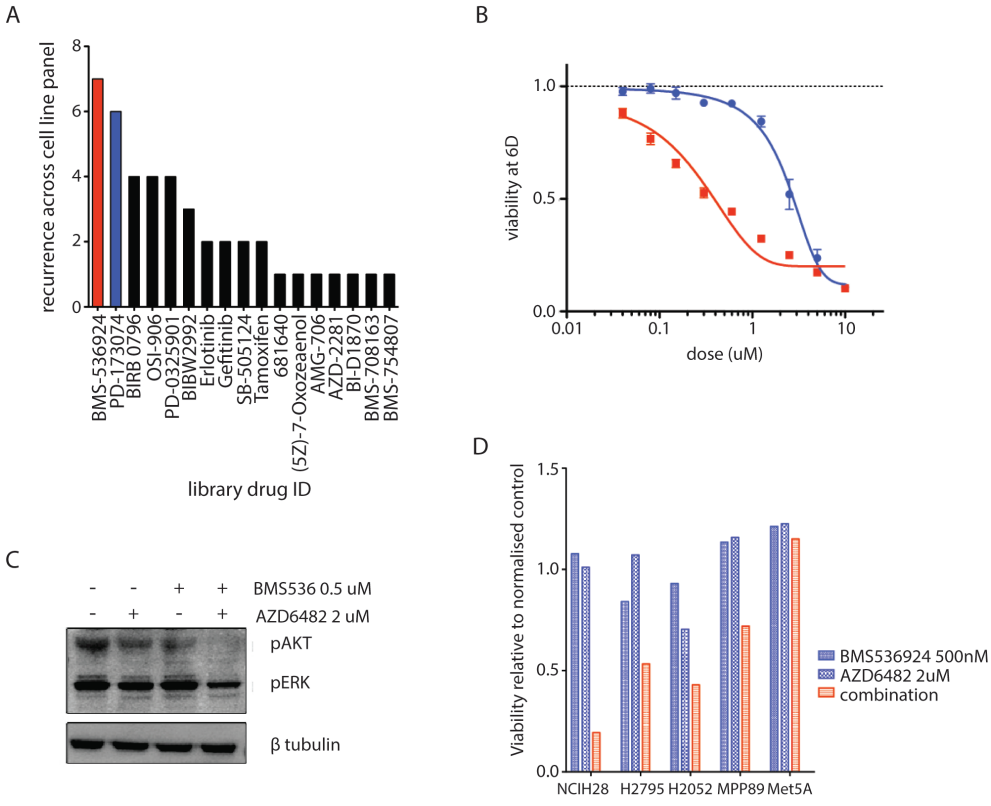


**Fig. S8. Combination drug screen of PI3Kinase inhibitor plus drug library in MPM cell lines. A)** Bar chart showing recurrent synergistic events in a combination screen PI3K inhibitor AZD6482 plus 95 small molecule inhibitors across 15 MPM cell lines. Most recurrent inhibitor PD-173074 (n= 6 cell lines). **B)** Validation of synergy between IGF1R inhibitor and PI3K inhibitor AZD4682 in NCO-H28 (FGFRi resistant cell line). Dose-response kinetics of BMS-536924 alone (blue) or with fixed dose (2uM) of AZD6482 (red). **C)** Immunoblot of NCI-H28 FGFRi resistant cell line treated with a combination of IGF1R inhibitor BMS-536924 and PI3L inhibitor AZD6482 showing loss of pAKT with combination treatment. **D)** Cell Titer Blue quantificantion of 2 week clonogenix survival assay of 5 MPM cell lines with EGF1R inhibitor B<S-536942 alone and in combination iwth PI3K inhibitor AZD6482.

**Table S1.** List of compounds used in the chemical inhibitor screen.

| Identifier | Name | Synonyms | Brand name | Action | Clinical Stage | Putative Target | Targeted process/pathway |
|---|---|---|---|---|---|---|---|
| 1 | Erlotinib | AY-22989, Sirolimus, WY-090217 | Tarceva | targeted | clinically approved | EGFR | EGFR signaling |
| 3 | Rapamycin | | Rapamune | targeted | clinically approved | MTOR | TOR signaling |
| 5 | Sunitinib | | Sutent | targeted | clinically approved | PDGFRA, PDGFRB, KDR, KIT, FLT3 | RTK signaling |
| 6 | PHA-665752 | zLLL | | targeted | experimental | MET | RTK signaling |
| 9 | MG-132 | BMS-181339-01 | | targeted | experimental | Proteasome | other |
| 11 | Paclitaxel | 11-deoxojervine | Taxol | cytotoxic | clinically approved | Microtubules | cytoskeleton |
| 17 | Cyclopamine | | | targeted | experimental | SMO | other |
| 29 | AZ628 | BAY-43-9006 | | targeted | experimental | BRAF | ERK MAPK signaling |
| 30 | Sorafenib | MK-045, MK-0457,VX-68 | Nexavar | targeted | clinically approved | PDGFRA, PDGFRB, KDR, KIT, FLT3 | RTK signaling |
| 32 | VX-680 | STI-571 | MK-0457 | targeted | in clinical development | AURKA, AURKB, AURKC, FLT3, ABL1, JAK2 | mitosis |
| 34 | Imatinib | KIN001-017 | Gleevec | targeted | clinically approved | ABL, KIT, PDGFR | ABL signaling |
| 35 | NVP-TAE684 | PF-02341066 | TAE684 | targeted | experimental | ALK | RTK signaling |
| 37 | Crizotinib | Saracatinib, KIN001-045 | Xalkori | targeted | in clinical development | MET, ALK | RTK signaling |
| 38 | AZD-0530 | NSC 83265 | | targeted | in clinical development | SRC, ABL1 | ABL signaling |
| 41 | S-Trityl-L-cysteine | Z-L-Norleucine-CHO | | targeted | experimental | KIF11 | mitosis |
| 45 | Z-LLNle-CHO | KIN001-005 | na | targeted | experimental | g-secretase | other |
| 51 | Dasatinib | KIN001-013 (GNF-2 / 3-(6-(4-(trifluoromethoxy) phenylamino)pyrimidin-4-yl) benzamide) | Sprycel | targeted | clinically approved | ABL, SRC, KIT, PDGFR | ABL signaling |
| 52 | GNF-2 | KIN001-019 | | targeted | experimental | ABL [T315I] | ABL signaling |

| Identifier | Name | Synonyms | Brand name | Action | Clinical stage | Putative target | Targeted process/pathway |
|---|---|---|---|---|---|---|---|
| 53 | GCP-60474 | CINK4, KIN001-021 | | targeted | experimental | CDK1, CDK2, CDK5, CDK7, CDK9 | |
| 54 | CGP-082996 | A770041, KIN001-111 | | targeted | experimental | CDK4 | cell cycle |
| 55 | A-770041 | KIN001-112 | A770041 | targeted | experimental | SRC family | other |
| 56 | WH-4-023 | KIN001-123 | | targeted | experimental | SRC family, ABL | ABL signaling |
| 59 | WZ-1-84 | KIN001-124 | | targeted | experimental | BMX | other |
| 60 | BI-2536 | KIN001-126 | NPK33-1-98-1 | targeted | in clinical development | PLK1, PLK2, PLK3 | mitosis |
| 62 | BMS-536924 | KIN001-127 | BMS-536924 | targeted | experimental | IGF1R | IGFR signaling |
| 63 | BMS-509744 | KIN001-128 | BMS-509744 | targeted | experimental | ITK | other |
| 64 | CMK | | Chloromethylketone Rsk inhibitor | targeted | experimental | RSK | ERK MAPK signaling |
| 71 | Pyrimethamine | | Daraprim | cytotoxic | clinically approved | Dihydrofolate reductase (DHFR) | DNA replication |
| 83 | JW-7-52-1 | KIN001-139 | | targeted | experimental | MTOR | TOR signaling |
| 86 | A-443654 | KIN001-134 | | targeted | experimental | AKT1, AKT2, AKT3 | PI3K signaling |
| 87 | GW843682X | MS275 | GW843682X (AN-13) | targeted | experimental | PLK1 | mitosis |
| 88 | MS-275 | | | targeted | in clinical development | HDAC | chromain histone acetylation |
| 89 | Parthenolide | KIN001-135 | | targeted | in clinical development | NFKB1 | other |
| 91 | KIN001-135 | | | targeted | experimental | IKKE | other |
| 94 | TGX221 | LDP-341, PS-341 | | targeted | experimental | PI3Kbeta | PI3K signaling |
| 104 | Bortezomib | XMD8-85 | Velcade | targeted | clinically approved | Proteasome | other |
| 106 | XMD8-85 | Seliciclib | | targeted | experimental | MAP2K5 (ERK5) | other |
| 110 | Roscovitine | 3-Phenyl-N-[2,2,2-trichloro-1-[[(8-quinolinylamino) thioxomethyl]amino]ethyl]-2-propenamide | | targeted | in clinical development | CDKs | cell cycle |
| 111 | Salubrinal | Tykerb, Tyverb | | targeted | experimental | GADD34-PP1C | other |

| | | | | | | | |
|---|---|---|---|---|---|---|---|
| 119 | Lapatinib | KIN001-155 | Tykerb, Tyverb | targeted | clinically approved | ERBB2, EGFR | EGFR signaling |
| 127 | GSK269962A | Doxil, Rubex | | targeted | experimental | ROCK1, ROCK2 | cytoskeleton |
| 133 | Doxorubicin | VP-16 | Adriamycin | cytotoxic | clinically approved | DNA intercalating | DNA replication |
| 134 | Etoposide | LY-188011 | Etophophos | cytotoxic | clinically approved | TOP2 | DNA replication |
| 135 | Gemcitabine | | Gemzar | cytotoxic | clinically approved | DNA replication | DNA replication |
| 136 | Mitomycin C | | | cytotoxic | clinically approved | DNA crosslinker | DNA replication |
| 140 | Vinorelbine | | Navelbine | cytotoxic | clinically approved | Microtubules | cytoskeleton |
| 147 | NSC-87877 | ICI-176334 | | targeted | experimental | PTPN6 (SHP-1), PTPN11 (SHP-2) | other |
| 150 | Bicalutamide | QS11 | Casodex | targeted | clinically approved | ANDR (androgen receptor) | other |
| 151 | QS11 | [2-(6,7-dimethoxyquinazolin-4-yl)-5-(pyridin-2-yl)-2H-1,2,4-triazol-3-amine] | | targeted | experimental | ARFGAP | other |
| 152 | CP466722 | PKC 412 | | targeted | experimental | ATM | Genome integrity |
| 153 | Midostaurin | CT 99021 | | targeted | in clinical development | KIT | RTK signaling |
| 154 | CHIR-99021 | KIN001-192 | | targeted | experimental | GSK3B | WNT signaling |
| 155 | AP-24534 | KIN001-193 | Ponatinib | targeted | in clinical development | ABL | ABL signaling |
| 156 | AZD6482 | KIN001-204 | | targeted | in clinical development | PI3Kbeta | PI3K signaling |
| 157 | JNK-9L | (KIN001-205) | | targeted | experimental | JNK | JNK and p38 signaling |
| 158 | PF-562271 | KIN001-206 | | targeted | experimental | FAK | cytoskeleton |
| 159 | HG-6-64-1 | JQ1 | | targeted | experimental | BRAFV600E, TAK, MAP4K5 | ERK MAPK signaling |
| 163 | JQ1 | JQ12 | | targeted | experimental | BRD4 | chromatin other |
| 164 | JQ12 | Dimethyloxalylglcine | | targeted | experimental | HDAC | chromain histone acetylation |
| 165 | DMOG | | | targeted | experimental | Prolyl-4-Hydroxylase | other |
| 166 | FTI-277 | AR-12 | | targeted | experimental | Farnesyl transferase (FNTA) | other |
| 167 | OSU-03012 | Shikonin | | targeted | experimental | PDPK1 (PDK1) | PI3K signaling |
| 170 | Shikonin | | | not defined | in clinical development | unknown | other |
| 171 | AKT inhibitor VIII | | | targeted | in clinical development | AKT1, AKT2, AKT3 | PI3K signaling |

| Identifier | Name | Synonyms | Brand name | Action | Clinical stage | Putative target | Targeted process/pathway |
|---|---|---|---|---|---|---|---|
| 172 | Embelin | FH535 | | targeted | in clinical development | XIAP | apoptosis regulation |
| 173 | FH535 | PAC-1 | | not defined | experimental | unknown | other |
| 175 | PAC-1 | IPA-3 | | targeted | in clinical development | CASP3 agonist | apoptosis regulation |
| 176 | IPA-3 | | | targeted | experimental | PAK1, PAK2, PAK3 | cytoskeleton |
| 177 | GSK-650394 | | | targeted | experimental | SGK3 | other |
| 178 | BAY 61-3606 | 5-Fluorouracil | | targeted | experimental | SYK | other |
| 179 | 5-Fluorouracil | | | cytotoxic | clinically approved | DNA antimetabolite | DNA replication |
| 180 | Thapsigargin | | | targeted | experimental | sarco-endoplasmic reticulum Ca2+-ATPases | other |
| 182 | Obatoclax Mesylate | | GX15-070 | targeted | in clinical development | BCL2, BCL2L1, MCL1 | apoptosis regulation |
| 184 | BMS-754807 | OSI-906 | | targeted | in clinical development | IGF1R | IGFR signaling |
| 185 | OSI-906 | LG-100069, LGD-1069 | | targeted | in clinical development | IGF1R | IGFR signaling |
| 186 | Bexarotene | | Targretin | targeted | clinically approved | Retinioic acid X family agonist | other |
| 190 | Bleomycin | DDE-28 | | cytotoxic | clinically approved | DNA damage | DNA replication |
| 192 | LFM-A13 | GW-2580 | | targeted | experimental | BTK | other |
| 193 | GW-2580 | VER-52296, NVP-AUY922 | | targeted | experimental | CSF1R (cFMS) | RTK signaling |
| 194 | AUY922 | Phenformin | | targeted | in clinical development | HSP90 | other |
| 196 | Phenformin | Bryostatin 1 | imidodica_ rbonimidi_c diamide_, N-(2-ph_enylethyl_)- | targeted | experimental | AAPK1 (AMPK) agonist | metabolism |
| 197 | Bryostatin 1 | GW786034 | NSC 339555 | targeted | in clinical development | PRKC | other |
| 199 | Pazopanib | Dacinostat, NVP-LAQ824 | Votrient | targeted | in clinical development | VEGFR, PDGFRA, PDGFRB, KIT | RTK signaling |
| 200 | LAQ824 | GNF-PF-193 | | targeted | in clinical development | HDAC | chromain histone acetylation |

| | | | | | | | |
|---|---|---|---|---|---|---|---|
| 201 | Epothilone B | GSK1904529A | EPO906 (ixabepilone, Patupilone) | cytotoxic | in clinical development | Microtubules | cytoskeleton |
| 202 | GSK-1904529A | | | targeted | experimental | IGF1R | IGFR signaling |
| 203 | BMS-345541 | | | targeted | experimental | IKBKB | other |
| 204 | Tipifarnib | Avagacestat | Zarnestra, IND58359, R115777 | targeted | in clinical development | Farnesyl-transferase (FNTA) | other |
| 205 | BMS-708163 | INCB-18424 | | targeted | in clinical development | g-secretase | other |
| 206 | Ruxolitinib | AS601245 | Jakafi | targeted | clinically approved | JAK1, JAK2, TYK2 | other |
| 207 | AS601245 | Ispinesib Mesylate | | targeted | experimental | JNK | JNK and p38 signaling |
| 208 | SB-715992 | | | targeted | in clinical development | KIF11 | mitosis |
| 211 | TL-2-105 | | | targeted | experimental | CRAF | ERK MAPK signaling |
| 219 | AT-7519 | KIN001-201 | | targeted | in clinical development | CDK9 | cell cycle |
| 221 | TAK-715 | KIN001-175 | | targeted | in clinical development | p38a | JNK and p38 signaling |
| 222 | BX-912 | KIN001-167 | | targeted | experimental | PDPK1 (PDK1) | PI3K signaling |
| 223 | ZSTK474 | KIN001-173 | | targeted | in clinical development | PI3K | PI3K signaling |
| 224 | AS605240 | | | targeted | experimental | PI3Kgamma | PI3K signaling |
| 225 | Genentech Cpd 10 | | | targeted | experimental | AURKA, AURKB | mitosis |
| 226 | GSK1070916 | | | targeted | in clinical development | AURKB | mitosis |
| 228 | KIN001-102 | Enzastaurin | | targeted | experimental | AKT1 | PI3K signaling |
| 229 | LY317615 | | | targeted | in clinical development | PRKCB (PKCbeta) | other |
| 230 | GSK429286A | KIN001-242 | | targeted | experimental | ROCK2 | cytoskeleton |
| 231 | FMK | | | targeted | experimental | RSK | ERK MAPK signaling |
| 235 | QL-XII-47 | | | targeted | experimental | BTK, BMX | other |
| 238 | CAL-101 | | | targeted | clinically approved | PI3Kdelta | PI3K signaling |

| Identifier | Name | Synonyms | Brand name | Action | Clinical stage | Putative target | Targeted process/pathway |
|---|---|---|---|---|---|---|---|
| 245 | UNC0638 | Cabozantinib | | targeted | experimental | G9a(EHMT2), GLP(EHMT1) | chromatin histone methylation |
| 249 | XL-184 | | Cometriq | targeted | clinically approved | VEGFR, MET, RET, KIT, FLT1, FLT3, FLT4, Tie2,AXL | RTK signaling |
| 252 | WZ3105 | | | targeted | experimental | CLK2, CNSK1E, FLT3, ULK1 | other |
| 253 | XMD14-99 | Quizartinib, AC-220 | | targeted | experimental | EPHB3, CAMK1 | RTK signaling |
| 254 | AC220 | | | targeted | in clinical development | FLT3 | RTK signaling |
| 255 | CP724714 | | | targeted | in clinical development | ERBB2 | EGFR signaling |
| 256 | JW-7-24-1 | | | targeted | experimental | LCK | other |
| 257 | NPK76-II-72-1 | | | targeted | experimental | PLK3 | mitosis |
| 258 | STF-62247 | | | not defined | experimental | stimulates autophagy | other |
| 260 | NG-25 | | | targeted | experimental | MAP3K7 (TAK1) | other |
| 261 | TL-1-85 | | | targeted | experimental | MAP3K7 (TAK1) | other |
| 262 | VX-11e | | | targeted | experimental | ERK | ERK MAPK signaling |
| 263 | FR-180204 | | | targeted | experimental | ERK | ERK MAPK signaling |
| 265 | Tubastatin A | | | targeted | experimental | HDAC6 | chromain histone acetylation |
| 266 | Zibotentan, ZD4054 | Sepantronium bromide | | targeted | in clinical development | Endothelin A Receptor | other |
| 268 | YM155 | XI-006 | | targeted | in clinical development | BIRC5 (Survivin) | apoptosis regulation |
| 269 | NSC-207895 | 4-(Butanoyloxymethyl) phenyl-(2E,4E,6E,8E)-3,7-dimethyl-9-(2,6,6-trimethylcyclohex-1-enyl) nona-2,4,6,8-tetraenoate | | targeted | experimental | MDM4 | p53 pathway |
| 271 | VNLG/124 | HDAC-42 | | targeted | experimental | HDAC, RAR | chromain histone acetylation |
| 272 | AR-42 | | | targeted | in clinical development | HDAC | chromain histone acetylation |

| | | | | | | |
|---|---|---|---|---|---|---|
| 273 | CUDC-101 | | targeted | in clinical development | HDAC, EGFR | chromain histone acetylation |
| 274 | PXD101, Belinostat | GSK525762A, | targeted | clinically approved | HDAC | chromain histone acetylation |
| 275 | I-BET 151 | | targeted | experimental | BRD2, BRD3, BRD4 | chromatin other |
| 276 | CAY10603 | | targeted | experimental | HDAC6 | chromain histone acetylation |
| 277 | ABT-869 | Linifanib | targeted | in clinical development | VEGFR and PDGFR family | RTK signaling |
| 279 | BIX02189 | | targeted | experimental | MAP2K5 (MEK5) | other |
| 281 | CH5424802 | | targeted | in clinical development | ALK | RTK signaling |
| 282 | EKB-569 | Pelitinib | targeted | in clinical development | EGFR | EGFR signaling |
| 283 | GSK2126458 | EX-8678 | targeted | in clinical development | PI3K, MTOR | PI3K signaling |
| 286 | KIN001-236 | | targeted | experimental | TIE2 | other |
| 287 | KIN001-244 | | targeted | experimental | PDPK1 (PDK1) | PI3K signaling |
| 288 | KIN001-055 | WHI-P97, AC1L1GQE | targeted | experimental | JAK3, MNK1 | other |
| 290 | KIN001-260 | Bayer IKKb inhibitor | targeted | experimental | IKK | other |
| 291 | KIN001-266 | | targeted | experimental | MAP3K8 (COT) | other |
| 292 | Masitinib | AB1010 | targeted | clinically approved | KIT | RTK signaling |
| 293 | MP470 | | targeted | in clinical development | PDGFR | RTK signaling |
| 294 | MPS-1-IN-1 | | targeted | experimental | MPS1 | mitosis |
| 295 | NVP-BHG712 | | targeted | experimental | EPHB4 | RTK signaling |
| 298 | OSI-930 | | targeted | in clinical development | KIT, VEGFR, PDGFR | RTK signaling |
| 299 | OSI-027 | activebiochem A-1065 | targeted | in clinical development | MTORC1/2 | TOR signaling |
| 300 | CX-5461 | | targeted | experimental | RNA Pol I | other |
| 301 | PHA-793887 | | targeted | experimental | CDK-pan | cell cycle |
| 302 | PI-103 | | targeted | experimental | PI3Ka, PRKDC (DNAPK) | PI3K signaling |
| 303 | PIK-93 | | targeted | experimental | PI4K, PI3K | PI3K signaling |

| Identifier | Name | Synonyms | Brand name | Action | Clinical stage | Putative target | Targeted process/pathway |
|---|---|---|---|---|---|---|---|
| 304 | SB52334 | | | targeted | experimental | ALK5 | RTK signaling |
| 305 | TPCA-1 | | | targeted | experimental | IKK | other |
| 306 | TG101348 | | | targeted | in clinical development | JAK2 | other |
| 308 | XL-880 | GSK1363089, foretinib | | targeted | in clinical development | MET | RTK signaling |
| 309 | Y-39983 | | | targeted | experimental | ROCK | cytoskeleton |
| 310 | YM201636 | | | targeted | experimental | FYV1 | other |
| 312 | AV-951 | Tivozanib | | targeted | in clinical development | VEGFR | RTK signaling |
| 326 | GSK690693 | | | targeted | experimental | AKT | PI3K signaling |
| 328 | SNX-2112 | | | targeted | experimental | HSP90 | other |
| 329 | QL-XI-92 | | | targeted | experimental | DDR1 | RTK signaling |
| 330 | XMD13-2 | | | targeted | experimental | RIPK | other |
| **331** | QL-X-138 | | | targeted | experimental | MNK2, PRKDC (DNAPK), MTOR, BTK, JAK3 | other |
| 332 | XMD15-27 | | | targeted | experimental | CAMK2B, CLK2, DYRK1A, MAST1, STK39 | other |
| 333 | T0901317 | | | targeted | experimental | LXR | other |
| 341 | EX-527 | | | targeted | experimental | SIRT1 | other |
| 344 | THZ-2-49 | | | targeted | experimental | CDK9 | cell cycle |
| 345 | KIN001-270 | | | targeted | experimental | CDK9 | cell cycle |
| 346 | THZ-2-102-1 | | | targeted | experimental | CDK7 | cell cycle |
| 1001 | AICAR | N1-(b-D-Ribofuranosyl)-5-aminoimidazole-4-carboxamide | AICAR | targeted | in clinical development | AAPK1 (AMPK) agonist | metabolism |
| 1003 | Camptothecin | 7-Ethyl-10-Hydroxy-Camptothecin,SN-38 | SN-38 | cytotoxic | clinically approved | TOP1 | DNA replication |
| 1004 | Vinblastine | Vinblastine sulphate | Vinblastine | cytotoxic | clinically approved | Microtubules | cytoskeleton |

| | | | | | | | |
|---|---|---|---|---|---|---|---|
| 1005 | Cisplatin | cis-Diammineplatinum(II) dichloride | Cisplatin | cytotoxic | clinically approved | DNA crosslinker | DNA replication |
| 1006 | Cytarabine | Ara-Cytidine, Arabinosyl Cytosine, U-19920 | Cytarabine (AraC) | cytotoxic | clinically approved | DNA synthesis | DNA replication |
| 1007 | Docetaxel | RP-56976 | Taxotere | cytotoxic | clinically approved | Microtubules | cytoskeleton |
| 1008 | Methotrexate | | Methotrexate | cytotoxic | clinically approved | Dihydrofolate reductase (DHFR) | DNA replication |
| 1009 | ATRA | Tretinoin | Vesanoid | targeted | clinically approved | Retinoic acid and retinoid X receptor agonist | other |
| 1010 | Gefitinib | ZD-1839 | Iressa | targeted | clinically approved | EGFR | EGFR signaling |
| 1011 | ABT-263 | | | targeted | in clinical development | BCL2, BCL2L1, BCL2L2 | apoptosis regulation |
| 1012 | Vorinostat | SAHA | Zolinza | targeted | clinically approved | HDAC inhibitor Class I, IIa, IIb, IV | chromain histone acetylation |
| 1013 | Nilotinib | | Tasigna | targeted | clinically approved | ABL | ABL signaling |
| 1014 | RDEA119 | RDEA119 | | targeted | in clinical development | MAP2K1 (MEK1), MAP2K2 (MEK2) | ERK MAPK signaling |
| 1015 | CI-1040 | PD-18435, PD-184352 | | targeted | in clinical development | MAP2K1 (MEK1), MAP2K2 (MEK2) | ERK MAPK signaling |
| 1016 | Temsirolimus | CCI-779 | Torisel | targeted | clinically approved | MTOR | TOR signaling |
| 1017 | Olaparib | KU-0059436, AZD-2281 | Lynparza | targeted | in clinical development | PARP1, PARP2 | Genome integrity |
| 1018 | ABT-888 | ABT-888 | | targeted | in clinical development | PARP1, PARP2 | Genome integrity |
| 1019 | Bosutinib | SKI-606 | Bosulif | targeted | clinically approved | SRC, ABL, TEC | ABL signaling |
| 1020 | Lenalidomide | | Revlimid | targeted | clinically approved | TNFA | other |
| 1021 | Axitinib | AG-013736 | Axitinib | targeted | in clinical development | PDGFR, KIT, VEGFR | RTK signaling |
| 1022 | AZD7762 | AZD 7762 | | targeted | in clinical development | CHEK1, CHEK2 | Genome integrity |
| 1023 | GW 441756 | | | targeted | experimental | NTRK1 | RTK signaling |
| 1024 | CEP-701 | CEP-701 | Lestaurtinib | targeted | in clinical development | FLT3, JAK2, NTRK1, RET | RTK signaling |
| 1025 | SB 216763 | SB 216763 | | targeted | experimental | GSK3A, GSK3B | WNT signaling |
| 1026 | 17-AAG | 17-AAG | Telatinib | targeted | in clinical development | HSP90 | other |
| 1028 | VX-702 | | | targeted | in clinical development | p38 | JNK and p38 signaling |

| Identifier | Name | Synonyms | Brand name | Action | Clinical stage | putative target | Targeted process/pathway |
|---|---|---|---|---|---|---|---|
| 1029 | AMG-706 | AMG-706 | | targeted | in clinical development | VEGFR, RET, c-KIT, PDGFR | RTK signaling |
| 1030 | KU-55933 | | Motesanib Diphosphate | targeted | experimental | ATM | Genome integrity |
| 1031 | Elesclomol | | | targeted | in clinical development | HSP70 | other |
| 1032 | Afatinib | Tovok, BIBW2992 | Gilotrif | targeted | clinically approved | ERBB2, EGFR | EGFR signaling |
| 1033 | Vismodegib | GDC-0449 | Erivedge | targeted | in clinical development | SMO | other |
| 1036 | PLX4720 | Vemurafenib (derivative) | Zelboraf (derivative) | targeted | clinically approved | BRAF | ERK MAPK signaling |
| 1037 | BX-795 | BX 795 | | targeted | in clinical development | TBK1, PDPK1, IKK, AURKB, AURKC | other |
| 1038 | NU-7441 | NU-7432,KU-57788 | | targeted | experimental | PRKDC (DNAPK) | Genome integrity |
| 1039 | SL 0101-1 | | | targeted | experimental | RSK, AURKB, PIM3 | ERK MAPK signaling |
| 1042 | BIRB 0796 | | Doramapimod | targeted | experimental | p38, JNK2 | JNK and p38 signaling |
| 1043 | JNK Inhibitor VIII | JNK Inhibitor VIII | | targeted | experimental | JNK | JNK and p38 signaling |
| 1046 | 681640,00 | 681640,00 | | targeted | experimental | WEE1, CHEK1 | cell cycle |
| 1047 | Nutlin-3a | Nutlin-3a (-) enantiomer | | targeted | in clinical development | MDM2 | p53 pathway |
| 1049 | PD-173074 | PD-173074 | | targeted | experimental | FGFR1, FGFR3 | RTK signaling |
| 1050 | ZM-447439 | ZM447439 | | targeted | experimental | AURKB | mitosis |
| 1052 | RO-3306 | | | targeted | experimental | CDK1 | cell cycle |
| 1053 | MK-2206 | | | targete | in clinical development | AKT1, AKT2 | PI3K signaling |
| 1054 | PD-0332991 | PD-0332991 | | targeted | in clinical development | CDK4, CDK6 | cell cycle |
| 1057 | NVP-BEZ235 | BEZ235 | | targeted | in clinical development | PI3K (Class 1) and MTORC1/2 | PI3K signaling |
| 1058 | GDC0941 | | | targeted | in clinical development | PI3K (class 1) | PI3K signaling |
| 1059 | AZD8055 | AZD8055 | pp242 | targeted | in clinical development | MTORC1/2 | TOR signaling |
| 1060 | PD-0325901 | PD-0325901 | | targeted | in clinical development | MAP2K1 (MEK1), MAP2K2 (MEK2) | ERK MAPK signaling |

| | | | | | | | |
|---|---|---|---|---|---|---|---|
| 1061 | SB590885 | | | targeted | experimental | BRAF | ERK MAPK signaling |
| 1062 | AZD6244 | | | targeted | in clinical development | MAP2K1 (MEK1), MAP2K2 (MEK2) | ERK MAPK signaling |
| 1066 | AZD6482 | WO2009093972 | | targeted | in clinical development | PI3Kbeta | PI3K signaling |
| 1067 | CCT007093 | | | targeted | experimental | PPM1D | other |
| 1069 | EHT 1864 | | | targeted | experimental | Rac GTPases | cytoskeleton |
| 1072 | BMS-708163 | Avagacestat | | targeted | in clinical development | g-secretase | other |
| 1091 | BMS-536924 | BMS-536924 | | targeted | experimental | IGF1R | IGFR signaling |
| 1114 | Cetuximab | Cetuximab | Erbitux | targeted | clinically approved | EGFR | EGFR signaling |
| 1129 | PF-4708671 | | | targeted | experimental | RPS6KB1 (p70S6KA) | TOR signaling |
| 1133 | JNJ-26854165 | | Serdemetan | targeted | in clinical development | MDM2 | p53 pathway |
| 1142 | HG-5-113-01 | | | targeted | in clinical development | LOK, LTK, TRCB, ABL(T315I) | ABL signaling |
| 1143 | HG-5-88-01 | | | targeted | experimental | EGFR, ADCK4 | EGFR signaling |
| 1149 | TW 37 | | | targeted | experimental | BCL2, BCL2L1 | apoptosis regulation |
| 1158 | XMD11-85h | | | targeted | experimental | BRSK2, FLT4, MARK4, PRKCD, RET, SPRK1 | other |
| 1161 | ZG-10 | | | targeted | experimental | IRAK1 | other |
| 1164 | XMD8-92 | | | targeted | experimental | MAP2K5 (ERK5) | other |
| 1166 | QL-VIII-58 | | | targeted | experimental | MTOR, ATR | TOR signaling |
| 1170 | CCT018159 | | | targeted | experimental | HSP90 | other |
| 1175 | AG-014699 | PF-01367338 | | targeted | experimental | PARP1, PARP2 | Genome integrity |
| 1192 | GSK269962A | KIN001-155 | | targeted | experimental | ROCK1, ROCK2 | cytoskeleton |
| 1194 | SB-505124 | 2-(5-Benzo[1,3]dioxol-5-yl-2-tert-butyl-3H-imidazol-4-yl)-6-methylpyridine hydrochloride hydrate | | targeted | experimental | TGFR1 (ALK5) | other |
| 1199 | Tamoxifen | | | targeted | clinically approved | ER | other |

| Identifier | Name | Synonyms | Brand name | Action | Clinical stage | Putative target | Targeted process/pathway |
|---|---|---|---|---|---|---|---|
| 1203 | QL-XII-61 | | | targeted | experimental | BTK | other |
| 1218 | JQ1 | | | targeted | experimental | BRD2, BRD3, BRD4 | chromatin other |
| 1219 | PFI-1 | | | targeted | experimental | BRD2, BRD3, BRD4 | chromatin other |
| 1230 | IOX2 | | | targeted | experimental | EGLN1 | other |
| 1236 | UNC0638 | | | targeted | experimental | G9a(EHMT2), GLP(EHMT1) | chromatin histone methylation |
| 1239 | YK 4-279 | | | targeted | experimental | RNA helicase A | other |
| 1241 | CHIR-99021 | CT 99021 | | targeted | experimental | GSK3B | WNT signaling |
| 1242 | (5Z)-7-Oxozeaenol | | | targeted | experimental | MAP3K7 (TAK1) | other |
| 1243 | piperlongumine | | | not defined | experimental | Increases ROS levels | other |
| 1248 | FK866 | APO866 | | targeted | experimental | NAMPT | metabolism |
| 1259 | BMN-673 | | | targeted | experimental | PARP1 | Genome integrity |
| 1261 | rTRAIL | | | targeted | experimental | TR10A (DR4), TR10B (DR5) | apoptosis regulation |
| 1262 | UNC1215 | | | targeted | experimental | LMBL3 | other |
| 1264 | SGC0946 | | | targeted | experimental | Q8TEK3 (DOT1L) | chromatin histone methylation |
| 1268 | XAV 939 | NVP-XAV 939 | | targeted | experimental | TNKS1 (tankyrase-1) | WNT signaling |
| 1371 | PLX4720 (rescreen) | Vemurafenib (derivative) | Zelboraf | targeted | experimental | BRAF | ERK MAPK signaling |
| 1372 | Trametinib | GSK1120212 | Mekinist | targeted | clinically approved | MAP2K1 (MEK1), MAP2K2 (MEK2) | ERK MAPK signaling |
| 1373 | Dabrafenib | GSK2118436 | Tafinlar | targeted | clinically approved | BRAF | ERK MAPK signaling |
| 1375 | Temozolomide | Temodar | | cytotoxic | clinically approved | DNA akylating agent | DNA replication |
| 1377 | Afatinib (rescreen) | Tovok, BIBW2992 | Gilotrif | targeted | clinically approved | ERBB2, EGFR | EGFR signaling |
| 1378 | Bleomycin (50 uM) | | | cytotoxic | clinically approved | DNA damage | DNA replication |
| 1494 | SN-38 | 7-ETHYL-10-HYDROXY-CAMPTOTHECIN | | cytotoxic | experimental | TOP1 | DNA replication |

| | | | | | | | | |
|---|---|---|---|---|---|---|---|---|
| 1495 | Olaparib | Olaparib | | targeted | clinically approved | PARP1, PARP2 | Genome integrity |
| 1498 | AZD6244 | | | targeted | in clinical development | MAP2K1 (MEK1), MAP2K2 (MEK2) | ERK MAPK signaling |
| 1502 | Bicalutamide | ICI-176334 | Casodex | targeted | clinically approved | ANDR (androgen receptor) | other |
| 1526 | RDEA119 (rescreen) | | | targeted | experimental | MAP2K1 (MEK1), MAP2K2 (MEK2) | ERK MAPK signaling |
| 1527 | GDC0941 (rescreen) | | | targeted | in clinical development | PI3K | PI3K signaling |
| 1529 | MLN4924 | | | targeted | in clinical development | NEDD8-activating enzyme | other |

**Table S2.** SPIA pathway analysis performed highlighting significantly upregulated/downregulated pathways between BAP1 mutant and BAP1 wild type lines.
Table size too big tio fit page. Available upon request

**Table S3.** GEO data analysis of 40 BAP1wt vs. 11 BAP1mt mesothelioma tumors showing fold change in mRNA expression

| ID | Adj. P value | P value | t | B | logFC | Gene symbol | Gene title |
|---|---|---|---|---|---|---|---|
| 206987_x_at | **0,0467** | 8,40E-06 | -4,9297914 | 2,074 | -1,55210916 | **FGF18** | fibroblast growth factor 18 |
| 211029_x_at | **0,0331** | 3,23E-06 | -5,200056 | 2,71569 | -1,46628317 | **FGF18** | fibroblast growth factor 18 |
| 211485_s_at | **0,0173** | 7,78E-07 | -5,5953934 | 3,66039 | -1,32935104 | **FGF18** | fibroblast growth factor 18 |
| 203638_s_at | 0,8387 | 9,17E-02 | -1,7172855 | -4,20483 | -0,58459186 | **FGFR2** | fibroblast growth factor receptor 2 |
| 208228_s_at | 0,8261 | 7,39E-02 | -1,822761 | -4,07017 | -0,57807812 | **FGFR2** | fibroblast growth factor receptor 2 |
| 205110_s_at | 0,7406 | 2,47E-02 | -2,3120189 | -3,35944 | -0,57359639 | **FGF13** | fibroblast growth factor 13 |
| 203639_s_at | 0,8385 | 8,69E-02 | -1,7439568 | -4,17143 | -0,42430659 | **FGFR2** | fibroblast growth factor receptor 2 |
| 204379_s_at | 0,7207 | 1,73E-02 | -2,4574403 | -3,12282 | -0,30363692 | **FGFR3** | fibroblast growth factor receptor 3 |
| 214284_s_at | 0,7144 | 8,97E-03 | -2,7123752 | -2,68264 | -0,2416635 | **FGF18** | fibroblast growth factor 18 |
| 215404_x_at | 0,7195 | 1,54E-02 | 2,5044305 | -3,04406 | 0,32050106 | **FGFR1** | fibroblast growth factor receptor 1 |